

Hydropyrolysis of Lignin using Pd/HZSM-5

Oliver D. Jan

A thesis
submitted in partial fulfillment of the
requirements of the degree of

Master of Science

University of Washington

2014

Thesis Committee:

Fernando Resende, Chair

Renata Bura

Richard Gustafson

Program Authorized to Offer Degree:
School of Environmental and Forest Sciences

©Copyright 2014
All Rights Reserved
Oliver D. Jan

University of Washington

Abstract

Hydropyrolysis of Lignin using Pd/HZSM-5

Oliver D. Jan

Chair of the Supervisory Committee:

Dr. Fernando Resende

School of Environmental and Forest Sciences

The aim of this work was to study the formation of cycloalkanes from hydropyrolysis of lignin with HZSM-5 and Pd/HZSM-5 catalysts. We observed that palladium supported on HZSM-5 catalyzed hydrogenation and deoxygenation reactions that converted phenolic compounds into aromatic hydrocarbons and cycloalkanes. This study analyzed the effect of the catalyst-to-lignin ratio, H₂ partial pressure, and temperature on the yields of hydrocarbons with HZSM-5 and Pd/HZSM-5. Pd/HZSM-5 produced 44% more aromatic hydrocarbons than HZSM-5 at a catalyst-to-lignin ratio of 20:1, 650°C, and a constant H₂ partial pressure of 1.7 MPa. The presence of palladium led to significant difference in yields only at 1.7 MPa H₂ partial pressure. In both the in-situ and ex-situ experiments conducted, hydropyrolysis temperature played a substantial role in the equilibrium conversion of hydrogenation reactions that led to cycloalkanes directly from lignin.

Dedication

This thesis is dedicated to my family for all their love and support

Acknowledgements

I would first like to express my thanks and gratitude towards my advisor and chair, Prof. Fernando Resende. His patience and willingness to teach me about reaction kinetics, thermodynamics, and even mortgages is something I will take with me for the rest of my professional career. Throughout the good moments and the stressful times, he remained positive and I believe it is his positive mindset that has helped guide this new laboratory in the right direction. Our discussions have always been pleasant and filled with interesting ideas about how the research and laboratory have been progressing, from minute things such as delayed orders to monumental progress to our reactor systems. In addition, I appreciate his acknowledgement towards my own research interests and giving me not only the opportunity to explore my ideas, but to put them into practice in the laboratory. This work in this thesis would not have been possible without his support and guidance and for that I am incredibly grateful. I will not forget yelling in the laboratory when the first cycloalkanes appeared on the computer screen and happily showing him the results. I look forward to pursuing the remainder of my Ph.D. with Fernando as my advisor.

I am also very thankful towards the rest of my committee, Prof. Renata Bura and Prof. Richard Gustafson, for their immense knowledge and support. They are very approachable and friendly, which has made my transition into graduate school very smooth and rewarding.

This work would not been possible without the help from my colleagues in the Resende group, Guanqun Luo and Kayla Sprenger. Thank you both for your great advice and friendship throughout graduate school so far. In addition, I would like to thank the numerous undergraduates who have assisted with the projects and development of our laboratory: Devin

Chandler, Austin Montgomery, Cameron McCallum, Aaron Lattanzi, Victoria Yuen, Daniel Suss Riter, Leandro Almeida, and Fernando Leite.

The results of this thesis would not have been possible without the amazing researchers and students at Wayne State University. I personally would like to thank Prof. Eranda Nikolla for helping with this project and giving excellent advice on this project when it was first proposed.

Most importantly, I want to express my deepest gratitude towards my family for their never-ending love and support. Thank you for being there for me, throughout the hard times and the good times. There is not enough room in this thesis to fully express how much I appreciate what you have done for me, and I am incredibly lucky to have been raised the hardest working parents I have ever known. I am also very fortunate to have such an inspirational little sister.

Table of Contents

Abstract	iii
Dedication	iv
Acknowledgements	v
List of Figures	ix
List of Tables	xi
CHAPTER 1 INTRODUCTION	1
1.1 Potential of Lignin	1
1.2 Hydropyrolysis	2
1.3 Thesis goals and direction	2
1.4 References	4
CHAPTER 2 LITERATURE REVIEW	6
2.1 Current state of energy	6
2.2 Lignocellulosic biomass and second generation biofuels	8
2.3 Fast pyrolysis of lignin	9
2.4 Zeolite catalysis	11
2.5 Bifunctional catalysis	12
2.6 Zeolites and monofunctional platinum	14
2.7 Bifunctional catalysis: Platinum group metals supported on zeolites	17
2.8 Bifunctional catalysis: Platinum group metals on other supports	18
2.9 Bifunctional catalysis: Other metals supported on zeolites	22
2.10 Bifunctional catalysis: Other metals supported on traditional supports	25
2.11 Summary	28
2.12 References	30
CHAPTER 3 MATERIALS AND EXPERIMENTAL METHODS	34
3.1 Lignin	34
3.2 Catalyst preparation	34
3.3 Hydropyrolysis-gas chromatography/mass spectrometry	35
3.4 Elemental Analysis	37
3.5 Data analysis	37
CHAPTER 4 RESULTS AND DISCUSSION	41
4.1 Lignin characterization	41
4.2 Noncatalytic hydropyrolysis of lignin	41
4.3 Catalytic hydropyrolysis of lignin	43
4.3.1. Effect of catalyst-to-lignin ratio	43
4.3.2. Effect of H ₂ partial pressure	46
4.3.3 Effect of Pd on product distribution	47
4.3.4. Effect of Temperature	49

4.4 Ex-situ hydrolysis of lignin	55
4.5 References	58
CHAPTER 5 THESIS SUMMARY AND FUTURE WORK.....	60
5.1 Thesis Summary.....	60
5.2 Future work	61
5.2.1 <i>Hydrolysis system</i>	61
5.2.2 <i>Ethylene-to-jet fuel system</i>	66
5.3 References	69

List of Figures

Figure 2-1. Lignin monomers: coumaryl alcohol, coniferyl alcohol, and syringyl alcohol	9
Figure 2-2. Van Krevelen diagram with differing H/C ratios as a function of O/C ratio for a variety of feedstocks	10
Figure 2-3. Visual representation of Pt atoms (pink) supported on HZSM-5; oxygen=red, aluminum=lavender, silicon=teal.....	13
Figure 2-4. Reaction network of HDO on 4-methylphenol with competitive deoxygenation and hydrogenation reactions [23]	14
Figure 2-5. Chemical structure of eugenol	15
Figure 2-6. Proposed reaction mechanism of guaiacol to cyclohexane with noble metal catalysts	20
Figure 2-7. Hydrodeoxygenation of phenolic monomers and dimers with Ni/HZSM-5.....	23
Figure 2-8. Common lignin linkages inherent in natural lignin.....	24
Figure 2-9. Octane numbers for common cycloalkane and aromatic compounds.....	25
Figure 2-10. Reaction mechanism of guaiacol conversion into benzene over Co/SiO ₂ compared to CoMo/Al ₂ O ₃	26
Figure 2-11. Guaiacol adsorption/reaction scheme predicted by Mochizuki et al.	27
Figure 2-12. Reaction pathways of β-O-4 cleavage through copper supported on alumina	27
Figure 3-1. Pyroprobe PFD. A: Pyroprobe, B: Packed bed reactor, C: In-line trap	35
Figure 4-1. Major phenolic and aromatic products produced from noncatalytic hydrolysis of lignin at 650°C	42
Figure 4-2. Effect of palladium on total aromatic hydrocarbon yield. Reaction conditions: T _{pyr} =650°C, P _H =1.72 MPa	44
Figure 4-3. Effect of palladium on phenolic yield. Reaction conditions: T _{pyr} =650°C, P _H =1.72 MPa.....	44
Figure 4-4. Effect of H ₂ partial pressure on aromatic hydrocarbon for HZSM-5 and Pd/HZSM-5. T=650°C, catalyst-to-lignin ratio: 20	47
Figure 4-5. Aromatic hydrocarbon distribution over HZSM-5 and Pd/HZSM-5 at 650°C, P _H =1.72 MPa, and 20:1 catalyst-to-lignin ratio	48
Figure 4-6. Chromatogram of catalytic hydrolysis of lignin at 400°C using Pd/HZSM-5....	50

Figure 4-7. Aromatic and cycloalkane yields with Pd/HZSM-5 at 400°C, 550°C, and 650°C at $P_H=1.72$ MPa.....	51
Figure 4-8. Hydrodeoxygenation reaction network of p-cresol to methylcyclohexane, adapted from Wang et. al.	52
Figure 4-9. Equilibrium constants for hydrogenation of various aromatic hydrocarbons [17]	54
Figure 4-10. Ex-situ upgrading of lignin into cycloalkane and aromatic compounds with Pd/HZSM-5 at varying packed bed reactor temperatures. Hydrogen partial pressure = 1.72 MPa, approximately 20:1 catalyst to lignin ratio held constant.....	55
Figure 4-11. Product distribution of cycloalkanes produced using Pd/HZSM-5. Conditions: back reactor T: 300°C, 20:1 catalyst to lignin ratio, hydrogen partial pressure: 1.72 MPa.....	56
Figure 5-1. Hydropyrolysis system PFD	62
Figure 5-2. Overall hydropyrolysis system complete with screw feeder, hydrogen manifold,gas booster.....	63
Figure 5-3. Biomass screw feeder and rotating auger with funnel and vibrating tabs.....	64
Figure 5-4. Hydrogen gas manifold with both low and high-pressure options	64
Figure 5-5. Fluidized bed reactor with vertical tube furnace connected to cyclone.	65
Figure 5-6. Ethylene to jet fuel PFD.....	66
Figure 5-7. ETG reactor system.....	68

List of Tables

Table 3-1. Hydrolysis products with and without catalysts.....	40
Table 4-1. Elemental analysis of poplar lignin, *=tested by ICP/OES, single run.....	41
Table 4-2. Equilibrium constants for aromatics hydrogenation to cyclohexane. Enthalpy of reaction measured in kJ/mol. *calculated using equation 1.....	54

CHAPTER 1

INTRODUCTION

1.1 Potential of Lignin

The lignin component of biomass is a potential feedstock for the production of fuels and chemicals. Lignin comprises nearly 15-30 wt.% of lignocellulosic biomass and is the second most abundant source of renewable carbon on earth, behind only cellulose [1]–[3]. It is also abundant as a waste product, with approximately 50 million tons of lignin separated annually from pulp and paper mills around the world [4],[5]. Advancements in cellulosic ethanol production in biorefineries will also lead to an accumulation of lignin, which must be separated from cellulose and hemicellulose for effective hydrolysis and fermentation processes [2], [6], [7]. Lignin accounts for approximately 40% of the total energy density of lignocellulosic biomass, making it an attractive option for fuel production [3]. Despite this potential, lignin is currently used as a low-grade fuel to produce steam and electricity [8]. If more efficient routes for lignin conversion were developed, it could become a sustainable and economical source of fuels and chemicals.

A major impediment for lignin transformation to fuels and chemicals, however, is the formation of char that occurs during thermal or chemical depolymerization of the bulk aromatic structure. Lignin is comprised of a macromolecular assembly of phenylpropanoid aromatic rings connected through carbon-carbon bonds and ether linkages, with the β -O-4 aryl ether bonds being the most dominant [9]. As the structure is largely aromatic, commodity chemicals such as toluene and p-xylene could theoretically be produced from lignin. However, these etherified linkages readily decompose into solid residues upon thermal or chemical treatment by radical-

induced polymerization of aromatic rings [9],[10]. This agglomeration impedes molecular diffusion and adsorption on the active sites of catalysts, eventually leading to catalyst deactivation and clogging in reactors.

1.2 Hydropyrolysis

Thermochemical processes, such as hydropyrolysis, have been relatively unexplored for the production of biofuels. Hydropyrolysis is a thermal degradation process in which biomass is pyrolyzed into monomeric and oligomeric units in the presence of H₂. The H₂ environment plays an important role in the production of hydrocarbons from lignin. H₂ has been proposed as a suitable reaction medium for reducing the amount of coke on catalytic active sites, which makes hydropyrolysis of lignin a suitable thermochemical process to minimize coke formation on catalytic surfaces [11]. However, the design of proper catalysts for lignin hydropyrolysis is critical, as lignin also contains oxygen functional groups that must be removed to produce a fuel with heating value similar to liquid fuel produced from crude oil and petroleum [1],[3]. Therefore, a catalyst that could simultaneously facilitate the removal of oxygen heteroatoms and the addition of hydrogen atoms and simultaneously promote hydrogenation/char reduction would be ideal.

1.3 Thesis goals and direction

Our goal is to synthesize a suitable catalyst for this chemical transformation. Bifunctional catalysts, comprised of supported metals on acidic zeolite catalysts, have been proposed to facilitate hydrogenation and deoxygenation reactions [12]–[16]. This reaction mechanism, known as hydrodeoxygenation (HDO), is an important reaction pathway for lignin valorization into molecules such as cycloalkanes and branched aliphatic compounds commonly seen in

conventional liquid fuels. A majority of the present research has attempted HDO of model lignin components, such as guaiacol and anisole, with bifunctional catalysts consisting of platinum and zeolite supports [17], [18]. However, incomplete HDO was observed in this work, as the product distribution consisted primarily of aromatic hydrocarbons and phenolic compounds. In addition, very little work has been performed on raw lignin in general, particularly for catalytic thermochemical processes. It seems clear that further studies on raw lignin are necessary.

Palladium is a highly active hydrogenation catalyst and the combination of palladium with acidic zeolite catalysts has not been previously tested under H₂ conditions. The addition of palladium to zeolite supports (Pd/HZSM-5) in H₂ may accelerate hydrogenation reactions necessary to facilitate complete HDO of phenolic lignin into cycloalkane compounds. Pd/HZSM-5 catalysts can be used as a model catalyst to understand hydrogenation mechanisms and allow for the design of new, inexpensive catalysts in the future.

In the present work, we performed hydrolysis of lignin with and without catalysts using a pyroprobe interfaced with a gas chromatograph/mass spectrometer (Py-GC/MS). For the catalytic experiments, the lignin was mixed with an acidic support and a supported metal catalyst, HZSM-5 and Pd/HZSM-5, respectively. We varied the catalyst-to-lignin ratio, H₂ partial pressure, and hydrolysis temperature to observe the relationship of each parameter to the yields of aromatic hydrocarbons and cycloalkanes. To the best of our knowledge, this is the first hydrolysis study on natural lignin to yield cycloalkanes and the first to demonstrate bifunctional behavior of Pd/HZSM-5 for HDO reactions.

1.4 References

- [1] G. W. Huber, S. Iborra, and C. Avelino, "Synthesis of transportation fuels from biomass: chemistry, catalysts, and engineering," *Chem. Rev.*, vol. 106, no. 9, pp. 4044–4098, 2006.
- [2] P. Azadi, O. R. Inderwildi, R. Farnood, and D. A. King, "Liquid fuels, hydrogen and chemicals from lignin: A critical review," *Renew. Sustain. Energy Rev.*, vol. 21, pp. 506–523, May 2013.
- [3] D. M. Alonso, S. G. Wettstein, and J. A. Dumesic, "Bimetallic catalysts for upgrading of biomass to fuels and chemicals.," *Chem. Soc. Rev.*, vol. 41, no. 24, pp. 8075–98, Dec. 2012.
- [4] M. Zhang, F. L. P. Resende, and A. Moutsoglou, "Catalytic fast pyrolysis of aspen lignin via Py-GC/MS," *Fuel*, vol. 116, pp. 358–369, Jan. 2014.
- [5] M. J. Roy, "Hydrodeoxygenation of Lignin Model Compounds via Thermal Catalytic Reactions," 2012.
- [6] M. Kleinert and T. Barth, "Towards a Lignin-cellulosic Biorefinery: Direct One-Step Conversion of Lignin to Hydrogen-Enriched Biofuel," *Energy & Fuels*, vol. 46, no. 7, pp. 1371–1379, 2008.
- [7] P. R. Patwardhan, R. C. Brown, and B. H. Shanks, "Understanding the Fast Pyrolysis of Lignin," *ChemSusChem*, vol. 4, pp. 1629–1636, 2011.
- [8] T. Nimmanwudipong, R. C. Runnebaum, S. E. Ebeler, D. E. Block, and B. C. Gates, "Upgrading of Lignin-Derived Compounds: Reactions of Eugenol Catalyzed by HY Zeolite and by Pt/ γ -Al₂O₃," *Catal. Letters*, vol. 142, no. 2, pp. 151–160, Dec. 2011.
- [9] D. D. Laskar, M. P. Tucker, X. Chen, G. L. Helms, and B. Yang, "Noble-metal catalyzed hydrodeoxygenation of biomass-derived lignin to aromatic hydrocarbons," *Green Chem.*, vol. 16, no. 2, p. 897, 2014.
- [10] Z. Ma, E. Troussard, and J. a. van Bokhoven, "Controlling the selectivity to chemicals from lignin via catalytic fast pyrolysis," *Appl. Catal. A Gen.*, vol. 423–424, pp. 130–136, May 2012.
- [11] B. C. Gates, *Catalytic Chemistry*. Wiley Series in Chemical Engineering, 1992.
- [12] I. Chorkendorff and J. W. Niemantsverdriet, *Concepts of Modern Catalysis and Kinetics*. Wiley-VCH, 2005.
- [13] H. Wang, J. Male, and Y. Wang, "Recent Advances in Hydrotreating of Pyrolysis Bio-Oil and Its Oxygen-Containing Model Compounds," *ACS Catal.*, vol. 3, no. 5, pp. 1047–1070, May 2013.

- [14] P. Barbaro, F. Liguori, N. Linares, and C. M. Marrodan, "Heterogeneous Bifunctional Metal/Acid Catalysts for Selective Chemical Processes," *Eur. J. Inorg. Chem.*, vol. 2012, no. 24, pp. 3807–3823, Aug. 2012.
- [15] M. Bejblová, P. Zámstný, L. Červený, and J. Čejka, "Hydrodeoxygenation of benzophenone on Pd catalysts," *Appl. Catal. A Gen.*, vol. 296, no. 2, pp. 169–175, Dec. 2005.
- [16] Q. Bu, H. Lei, A. H. Zacher, L. Wang, S. Ren, J. Liang, Y. Wei, Y. Liu, J. Tang, Q. Zhang, and R. Ruan, "A review of catalytic hydrodeoxygenation of lignin-derived phenols from biomass pyrolysis," *Bioresource Technology*, vol. 124, pp. 470–477, 2012.
- [17] T. Nimmanwudipong, C. Aydin, J. Lu, R. C. Runnebaum, K. C. Brodwater, N. D. Browning, D. E. Block, and B. C. Gates, "Selective Hydrodeoxygenation of Guaiacol Catalyzed by Platinum Supported on Magnesium Oxide," *Catal. Letters*, vol. 142, no. 10, pp. 1190–1196, Aug. 2012.
- [18] X. Zhu, L. L. Lobban, R. G. Mallinson, and D. E. Resasco, "Bifunctional transalkylation and hydrodeoxygenation of anisole over a Pt/HBeta catalyst," *J. Catal.*, vol. 281, no. 1, pp. 21–29, Jul. 2011.

CHAPTER 2 LITERATURE REVIEW

2.1 Current state of energy

Fossil fuels have been the dominant source of transportation energy and electrical power generation in modern society. Global energy usage in 2006 reached 460 exajoules (1 EJ=10¹⁸ J), of which 87% were from fossil fuel consumption of petroleum, coal, and natural gas [1]. The United States alone consumed nearly 100 EJ, 85% of which came solely from fossil fuels, including the average consumption of nearly 7 x 10⁹ boe/year (boe/year = barrels of oil equivalent/year)[1], [2]. Electricity is a vital player in the energy market, with electricity usage taking 40% of the total energy consumption in the United States. Coal and natural gas make up 40% and 20% of the electricity usage respectively [1]. By 2050, it is expected that this energy consumption will double with the development of technology and society as a whole [3].

This rapid consumption and reliance on fossil fuels directly represents their immediate impact on the energy future of the United States. Unfortunately, the rate of consumption of fossil fuels is far greater than the rate of regeneration, which will lead to an impending depletion of these critical resources. Lifetime estimates for oil, coal, and natural gas are roughly 40, 80, and 100 years respectively [1]. It is estimated that the world's population will increase nearly 25% from 2010 to 2040 to more than 9 billion people, adding additional strain on limited fossil fuel resources.

Additionally, fossil fuel consumption is the main contributor of greenhouse gases and presents a difficult environmental problem. The United States Department of State observed that electricity, transportation, and industry accounted for 38%, 31%, and 14% of the CO₂ generation

in the United States respectively [4]. The quantity and rate of CO₂ emissions from fossil fuels is far greater than the rate at which it can be recaptured by plants and soils, leading to an increased rate of global warming and many other environmental problems [1], [3]. As a result of this impending depletion of fossil fuels and the environmental impact of these materials, it is necessary to research and develop alternative sources of energy that are efficient, sustainable, and environmentally benign. Several energy systems, such as nuclear, wind, solar, geothermal, and biomass have been proposed as leading candidates for alternative pathways for sustainable energy and fuel. While a majority of these technologies will be advantageous for electricity production, there is a vast population that require liquid fuels for transportation purposes.

Existing biofuels in the current market are termed "first generation" due to the conversion of corn, soybeans, and sugar cane, i.e, consumable agricultural crops, into bioethanol and biodiesel [5]. However, these feedstocks compete directly with the food industry and pose ethical questions in using food as a source of energy. However, lignocellulosic biomass ("second generation biofuels") is widely abundant and does not compete with the food industry, making them a viable option for liquid fuel production.

2.2 *Lignocellulosic biomass and second generation biofuels*

Lignocellulosic biomass is an attractive resource for the production of alternative transportation fuels as a result of its abundance and relatively low price. The United States Department of Agriculture and Oakridge National Laboratory estimates that the United States can produce a sustainable 1.3 billion metric tons of dry biomass per year, which is approximately 3.8×10^9 boe/year [2]. This target is more than half of the current consumption by the United States (7×10^9 boe/year).

“Second generation” biofuels are derived from nonedible, lignocellulosic feedstocks (corn stover, sugarcane bagasse, wheatstraw), wastes (paper, manure, lignin residues), and energy crops (miscanthus, willow, switchgrass, hybrid poplar) [3]. These feedstocks are mostly composed of three different compounds: cellulose, hemicellulose, and lignin, each differing significantly from one another in terms of structure, composition, and prevalence in softwoods/hardwoods and agricultural crops.

Cellulose is a polymer of glycosidically linked glucose units that can reach polymer chain lengths of 10,000-15,000 glucopyranose units [2]. Hemicellulose is an amorphous polymer that is composed of a random distribution of five-carbon (xylose, arabinose) and six-carbon sugars (glucose, galactose, and mannose). Both cellulose and hemicellulose make up nearly 60-90 wt% of biomass and are valuable feedstocks for fermentation to ethanol processes [2].

Lignin is found dispersed between cellulose and hemicellulose, providing protection and rigidity against decay, biological degradation, and climate [6]. It is also known colloquially as

the "glue" that holds cellulose and hemicellulose together. Lignin makes up nearly 15-30 wt% of biomass and, behind cellulose, it is the second most abundant source of renewable carbon on earth [2], [6], [7]. Although a definite polymeric structure of lignin has yet to be determined, approximate analyses indicate that lignin is composed of units of *p*-hydroxyphenol (H), guaiacyl (G), and syringyl (S), with each existing in differing proportions depending on the lignocellulose source [5], [8]. Their chemical structures are shown in Figure 2-1. They each differ by the number of methoxy groups adjacent to the hydroxyl group.

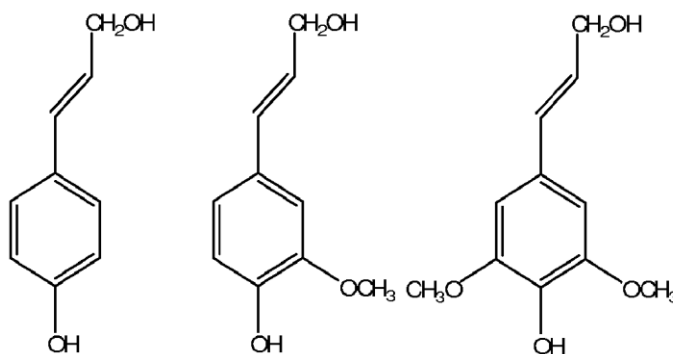


Figure 2-1. Lignin monomers: coumaryl alcohol, coniferyl alcohol, and syringyl alcohol

2.3 Fast pyrolysis of lignin

Thermochemical routes, such as pyrolysis, have been suggested as an economical process to convert waste lignin into a liquid product that is known as "bio-oil". Fast pyrolysis is the thermochemical decomposition of biomass in the absence of oxygen at 400-600°C and short residence times that produces a viscous, corrosive liquid that contains many oxygenated compounds. In order for bio-oil to be comparable to fossil fuel-derived oil, it must be upgraded

even further to remove excess oxygen to improve its heating value and miscibility with existing fuels [2].

Lignin has the highest specific energy density out of lignocellulose when comparing the oxygen to carbon (O/C) ratios of lignin to that of cellulose on a Van Krevelen diagram in Figure 2-2 [5], [6], [9]. However, even with this tremendous potential, lignin has not been pursued as a feedstock for biofuels production due to its complex array of interunit linkages, char formation, as well as poor product selectivity [1], [2], [6], [9]. As a result of its complex structure, lignin is treated as a waste product that is usually separated and burned off through a recovery boiler to be converted into electricity [2], [6], [8].

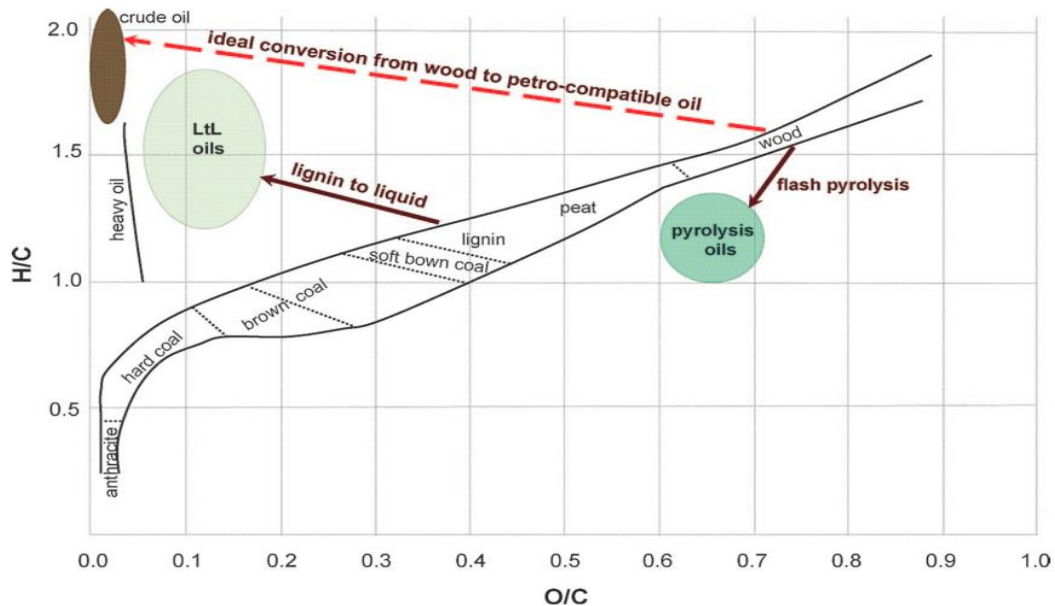


Figure 2-2. Van Krevelen diagram with differing H/C ratios as a function of O/C ratio for a variety of feedstocks

2.4 Zeolite catalysis

The catalytic pyrolysis of lignin has been analyzed using acidic zeolites for deoxygenation reactions to remove unwanted oxygen. Zeolites are defined as microporous crystalline solids, normally linked by SiO_4 and AlO_4 tetrahedra bonded through common oxygen atoms in a lattice framework [10], [11]. They are critical catalytic materials due to their high surface area, thermal resistance, solid-state acidity, adsorption capability, and steric selectivity as a result of their network of micropores (<2 nm OD) and mesopores (2-50 nm OD) [10], [12]–[16]. Zeolites can be converted into acidic solids by exchanging protons (H^+) into the framework to balance the Al^{3+} and Si^{4+} charges. Therefore, the acidity is proportional to the aluminum content of the zeolite, which makes zeolites tunable to specific applications depending on their synthesis.

HZSM-5 is an industrial zeolite catalyst that features a small pore size diameter compared to other zeolites such as Y zeolites and Zeolite beta. HZSM-5 has been previously studied to be the best catalyst for upgrading bio-oil as it produced the highest volume of liquid products and had low coke deposition through ex-situ catalytic upgrading [10], [17]. Ex-situ upgrading occurs when pyrolysis vapors are swept into a secondary unit for upgrading. However, mass transfer limitations exist due to the small pore size, allowing for the possibility for low catalytic efficiency. As a result, increasing pore accessibility can lead to higher mass transfer of reactant molecules to the highly dense active sites, thereby increasing the catalytic potential of these materials [10].

2.5 *Bifunctional catalysis*

Bifunctional heterogeneous catalysts refer to the assembly consisting of the support and the supported metal when both participate in a reaction [18]. Pt/Al₂O₃ is a common bifunctional catalyst in the petroleum industry in which the platinum metal facilitates hydrogenation reactions while the acidic alumina support performs isomerization/cracking reactions. The benefits of having this type of catalyst include having fewer unit operations (fewer catalytic reactors) and higher selectivity of certain products. Also, the introduction of metal nanoparticles as "nanocatalysts" also has unique benefits such as a much higher surface to volume ratio compared to a bulk metal. This translates to having a larger fraction of active sites exposed on the surface, potentially leading to higher catalytic activity compared to their bulkier analogs [19].

However, one of the problems with using bifunctional catalysts is the coke formation that slowly deactivates the catalyst over time, gradually reducing its effectiveness. Another issue with these catalysts is sintering at higher temperatures. Sintering is the agglomeration of particles into more thermodynamically favorable clusters of metal [3], [7], [12]. However, a way to prevent sintering and aggregation is to "anchor" the catalysts within void spaces of zeolites, metal oxides, and other support frameworks [19]. It is hypothesized that a synergistic relationship can exist between these types of supported bifunctional catalysts in which the metal and the support exhibit enhanced reactivity [7], [10], [14], [19]–[22]. Several of these studies show that the physical and chemical properties of the support and the metal contribute to overall improved catalytic performance that can reduce char formation [19]. An optimized structure of platinum supported on HZSM-5 is portrayed in Figure 2-3 [22].

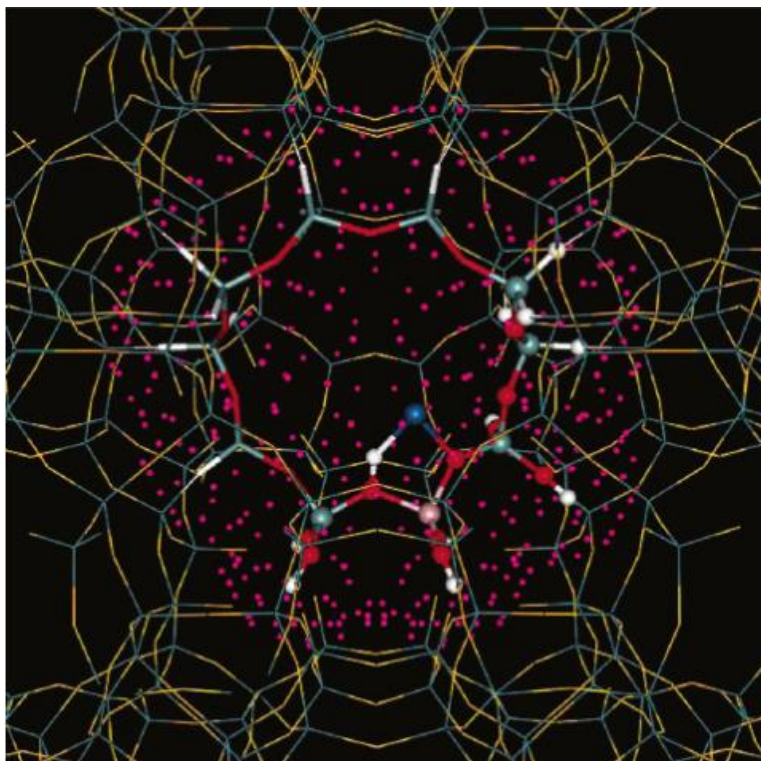


Figure 2-3. Visual representation of Pt atoms (pink) supported on HZSM-5; oxygen=red, aluminum=lavender, silicon=teal

Bio-oils derived from lignin are not suitable for use as liquid fuel mainly because of the high oxygen content present in the liquid. It is of great interest to optimize deoxygenation and hydrogenation reactions through a bifunctional route that can utilize the deoxygenation capability of a support and the hydrogenation ability of a metal in a bifunctional manner. This reaction mechanism is known as hydrodeoxygenation and is shown in Figure 2-4 with the hydrodeoxygenation of 4-methylphenol [23]. Deoxygenation (DDO) and hydrogenation (HYD) have differing rates, and different catalysts will promote DDO or HYD as a primary reaction depending on the nature of the metal and the support [10]. It has been observed that noble metals favor HYD whereas sulfided catalysts preferentially undergo DDO reactions [23], [24].

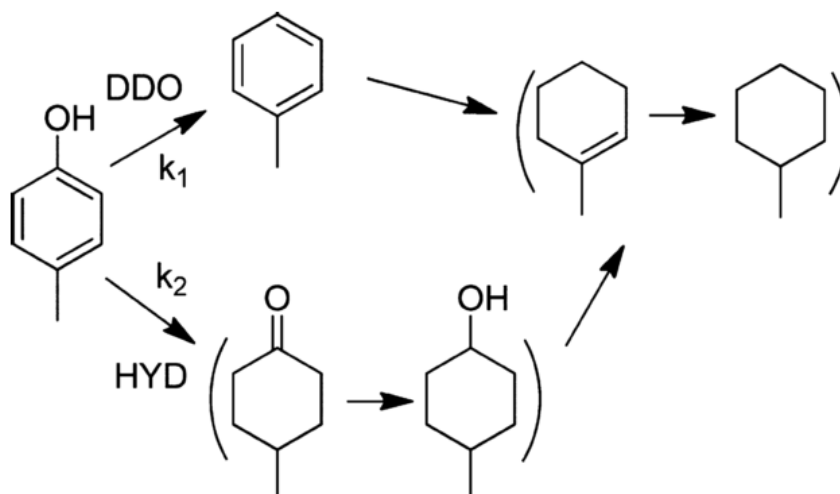


Figure 2-4. Reaction network of HDO on 4-methylphenol with competitive deoxygenation and hydrogenation reactions [23]

In addition to facilitating multiple reactions, an ideal bifunctional catalyst should still be able to exhibit a high turnover frequency (TOF) and the capability to maintain this activity after repeated trials.

The remainder of this paper focuses on published work regarding the use of bifunctional catalysts in upgrading lignin pyrolysis products. The analysis will focus on correlating product distribution with the type of metal, type of support, partial pressure of hydrogen, and temperature among others. A majority of the publications relating to lignin conversion focus on model compounds such as phenol and guaiacol in mostly batch catalytic systems. Some authors explore downstream upgrading of idealized pyrolysis vapors and bio-oil through fixed bed reactors.

2.6 Zeolites and monofunctional platinum

The catalytic behavior of zeolitic supports has garnered attention due to their solid acidity and size-restrictive pores. The Gates group at UC Davis analyzed eugenol conversion in HY zeolite. Eugenol was chosen because it matched closely to the structure of coniferyl alcohol

commonly found in natural lignin. Eugenol also provides three useful functional groups: a hydroxyl (-OH), methoxyl (-OCH₃), and an allyl (-CH₂-CH=CH₂), as shown in Figure 2-5.

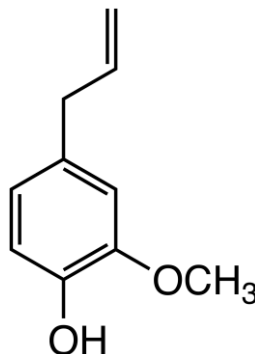


Figure 2-5. Chemical structure of eugenol

It was observed that, at 300°C and 20 psi, the major products were cis/trans-isoeugenol enantiomers through isomerization reactions [8]. These results may indicate unfavorable adsorption of the phenolic ring onto the Brønsted acid sites due to the sterically hindering alkenyl group. The authors also hypothesized that deallylation was a major reaction class due to the formation of guaiacol. Isomerization and deallylation occurred independent of hydrogen partial pressure, which indicated that hydrogen transfer reactions occurred primarily due to Brønsted acid interactions [8].

The Resasco group at the University of Oklahoma studied the effects of passing vaporized anisole (methoxybenzene) over HZSM-5 and HBeta catalysts to study the reaction pathways of the methoxy (-OCH₃) group during lignin pyrolysis [13], [14]. It was observed that the major reaction pathways of both zeolites were transalkylation reactions occurring from hydrogenolysis of the methoxy group, resulting in phenol, cresols, and xylenols. The authors hypothesize that the Brønsted acid sites in the two zeolites are responsible for these reactions. Additionally, the two catalysts shared minor pathways forming phenol and methylanisoles from

disproportionation reactions.

The authors mention that both HZSM-5 and HBeta were not effective deoxygenation catalysts largely due to the potential steric hindrance between anisole and the pore size of the zeolite. However, these structures did account for shape selectivity of methylanisoles, where *p*-methylanisole accounted for the majority isomer produced over HZSM-5 [13].

Along with the HBeta work done in [14], Zhu et al. experimented using platinum supported on SiO₂ to understand the behavior of anisole over platinum. To prove that the silica support was inactive, it was observed that only 2% conversion occurred over the support at maximum temperature (400°C) and space-time (4 hr). At lower W/F ratios with Pt/SiO₂, (catalyst weight/organic feed mass flow rate), demethylation reactions were the primary reaction as observed by the evolution of methane [14]. At increasing W/F, benzene and cyclohexane began to form, eventually reaching complete HDO at around 4 hours. Under the reaction conditions tested (400°C at atmospheric pressure), HDO was the dominant reaction pathway, representing that platinum is a valuable catalyst for HDO, dehydrogenation, and hydrogenation reactions in the presence of H₂.

However, the authors expect that the C_{aromatic}-OH bond does not undergo direct hydrogenolysis due to its immense bond strength compared to the C_{aliphatic}-OH bond (84 kJ/mol difference). The difference between the two situations is due to the electron delocalization of oxygen lone pairs into the π orbitals of the phenolic ring. It is hypothesized that there is partial hydrogenation near the C_{aromatic}-OH bond, resulting in decreased delocalization and subsequent dehydration to form benzene and water.

Additionally, in terms of stability testing between HBeta and Pt/SiO₂ for coke formation,

HBeta formed the highest degree of coke mainly due to its acidity and ability for methyl transfer reactions. This will be revisited in the following section when discussing a bifunctional Pt/HBeta catalyst that the authors tested.

2.7 *Bifunctional catalysis: Platinum group metals supported on zeolites*

Lignin bio-oil upgrading via platinum group metals (PGM) supported on zeolites have shown unique chemical transformations. Zhu et al., synthesized a bifunctional catalyst consisting of platinum particles supported on HBeta and observed a synergistic relationship that provided several enhancements over using each catalyst separately in anisole upgrading [14]. Several of these improvements came in the form of kinetically-driven reactions: transalkylation and HDO reaction rates improved by a notable increase in the rate of demethoxylation which may indicate an improved overall rate of Brønsted acid catalyzed methylation reactions. Enhanced stability and moderate reduction of coke formation were some of the other notable improvements of the bifunctional catalyst over the monofunctional HBeta and Pt/SiO₂ catalysts [14].

Another benefit of improved transalkylation is the minimization of carbon loss as methanol through demethylation [13], [14]. Instead, the methyl groups were retained and participated in transalkylation reactions within the bifunctional Pt/HBeta catalyst. The authors note that decreasing the metal content from 1.0% Pt to 0.2% Pt showed a marked increase in the formation of toluene, xylenes, and C₉ aromatics, suggesting that the product distribution can be altered by varying the metal/acid balance [14].

In addition to anisole, similar experiments were performed with phenol, cresols, guaiacol, and eugenol over Pt/Zeolite-Beta by Horacek et al. The authors also varied the Si/Al ratio of the zeolite support to determine the effects of Brønsted acidity on conversion [25]. Mild reaction

conditions compared to previous tests, with temperatures at 180°C and hydrogen pressure set to 5 MPa, points to this reaction as more of a downstream upgrading process rather than as an in-situ catalytic fast pyrolysis unit operation. It was observed that substituted phenolics, such as cresols (methylphenols), guaiacol (methoxyphenol), and eugenol (4-allyl-2-methoxyphenol) showed increasingly lower selectivity to combined hydrogenation and deoxygenation reactions as a result of limited access to platinum active sites [25]. This bulkiness factor has occurred for the case of eugenol in HY zeolite as previously mentioned [8]. However, in the case of phenol and cresol, a higher Si/Al ratio (20-22 versus 10-12) through dealumination resulted in higher rates of conversion. The authors speculate that this is due to the increased mass transfer of phenol and cresol in the pore structure [25].

It is interesting to note that the hydrogenation, hydrogenolysis reactions of methoxy groups on anisole reviewed earlier did not occur with guaiacol [14]. Horacek et al. hypothesized that this discrepancy is due to the presence of another substituent on the aromatic ring which hinders the adsorption on active sites on Brønsted acid sites and platinum sites. This has also been previously explored with eugenol and its bulky alkenyl functional group [8], [25].

Platinum supported on USY-zeolite used for the hydrogenation of benzene showed higher turnover numbers than traditional supports such as titania and alumina [26]. The authors explain that this phenomena might be related to platinum forming clusters inside the zeolite cage instead of having high dispersity throughout the structure. Interactions between these clusters and strong Brønsted acid sites of the zeolite form electron deficient platinum atoms, leading to enhanced hydrogenation and improved sulfur tolerance [26].

2.8 *Bifunctional catalysis: Platinum group metals on other supports*

Bifunctional catalysts with PGM have been tested on a variety of supports such as silicates [15], [27], aluminates [8], [28], [29], and carbon-based structures [30]–[32]. Additionally, bifunctional catalysts have been tested for nonphenolic compounds such as 2-methyl-2-pentenal with Pt, Pd, Cu on silica [14] and furfural on Pd/Al₂(SiO₃)₃ [21].

Research conducted by Lee et al. examined bifunctional catalysis of guaiacol into cyclohexane using major PGM such as platinum, rhodium, and palladium. The supports included alumina (Al₂O₃), silica-alumina (SiO₂-Al₂O₃), and nitric acid treated carbon (NAC). Catalytic reactions of guaiacol with an iteration of a supported metal catalyst were performed in a batch reactor at around 580 psi of H₂, 250°C, and residence time of 1 hour. It was observed that complete conversion was achieved for all catalyst iterations except Pt/SiAl (50%) and Pd/NAC (54%), with cyclohexane yields ranging from 14-60% [27]. The authors determined that the degree of HDO was strongly dependent on the acidity and number of active sites of the support. NAC-supported catalysts had the lowest cyclohexane selectivity, favoring products such as cyclohexanol and 2-methoxycyclohexanol. This observation indicated that carbon supports are not acidic and are not capable of performing deoxygenation reactions [27].

Additionally, the HDO activity of a Rh/silica-alumina bifunctionalized catalyst was higher than that of their monofunctional substituents. Silica-alumina supports displayed negligible guaiacol conversion while Rh supported on inactive, nonporous zirconia displayed excellent hydrogenation activity (methoxycyclohexanol formation) but negligible deoxygenation activity. The authors explain that this indicates that hydrogenation is linked to metal nanoparticle activity whereas the acidic sites on the support are required for deoxygenation reactions to occur. The mechanism that the authors rationalized from these results (Figure 2-6) showed the

hydrogenation of guaiacol into 2-methoxycyclohexanol, with subsequent demethoxylation to cyclohexanol and cyclohexanone, with further deoxygenation into cyclohexane through dehydration reactions [27].

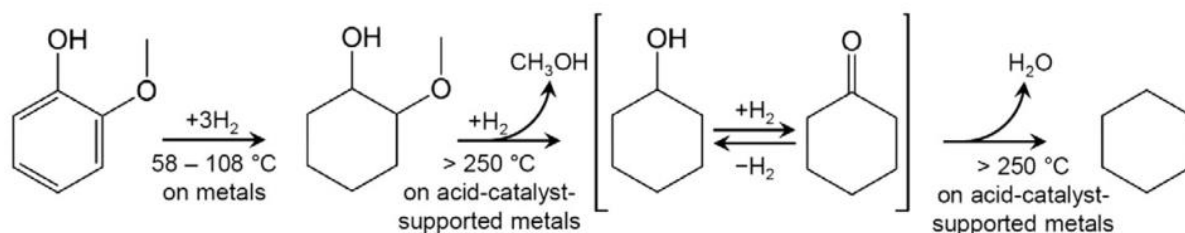


Figure 2-6. Proposed reaction mechanism of guaiacol to cyclohexane with noble metal catalysts

This work complements the guaiacol conversion work done by Nimmanwudipong et al. over $\text{Pt}/\gamma\text{-Al}_2\text{O}_3$. Experimental conditions were at 300°C and roughly 20.3 psi of pressure in the presence of hydrogen. It was observed that hydrogenolysis, deoxygenation, and hydrogenation were catalyzed by platinum metal while alumina was responsible for transalkylation reactions [28]. The degree of overall HDO was also determined to be highly dependent on the partial pressure of hydrogen. Similar results were observed by Runnebaum et al. using the same catalyst over other lignin-derived compounds (guaiacol, anisole, 4-methylanisole, and cyclohexanone) at the exact conditions [29].

Catalytic upgrading experiments on eugenol were also conducted by using similar alumina supports with platinum [8] at 300°C and atmospheric pressure. As noted previously with their work with HY zeolite, hydrogenation of the large alkenyl group of eugenol to 4-propylguaiacol was the predominant hydrogenation product with $\text{Pt}/\gamma\text{-Al}_2\text{O}_3$. However, steric hindrance adversely affected reagent adsorption on active Pt and alumina sites, resulting in a minimal conversion of HDO products [8]. The addition of hydrogen gas at atmospheric pressure

showed very little role in affecting the overall HDO of eugenol, further implying the effects of this "bulkiness" factor at these operating conditions. **Overcoming these steric limitations would be absolutely necessary for catalytic upgrading of natural lignin, which will not be neatly fragmented into monomers and dimers.**

Other mesoporous silicates such as SBA-15, tested by Lu et al. [15], were used as supports for palladium for the pyrolysis of poplar. Py-GC/MS was used to perform microscale pyrolysis and to analyze pyrolysis vapors through GC/MS at 600°C, holding time of 10 seconds, with He carrier gas. This experiment was done without hydrogen and the actual pyrolysis temperature was closer to 500°C due to heat transfer limitations of the pyroprobe. It was observed, for heterogeneous poplar, that the phenolic fraction increased with the addition of Pd to the zeolitic framework by promoting thermal cracking reactions. It is hypothesized that full conversion of phenolics and other oxygenated compounds to naphthenes and paraffins were not achieved due to steady catalyst deactivation over time and the lack of hydrogen partial pressure, resulting in limited hydrodeoxygenation [28]. Marked improvements in decarbonylation and hydrotreating were observed by the increase in monomeric phenol and decrease in aldehydes. These are important results as this can show that Pd/SBA-15 can result in a decrease in bio-oil viscosity due to the decreased oxygen content, thus resulting in an improved fuel with higher heating value [15]. Decarbonylation is an important catalytic reaction as aldehydes are responsible for aging and instability of bio-oils. Additionally, Pd/SBA-15 increased the yields of benzene, ethylbenzene, xylenes, and other aromatic molecules compared to monofunctional SBA-15.

2.9 Bifunctional catalysis: Other metals supported on zeolites

Other metals besides PGM supported on zeolites have also been explored as potential catalysts for lignin upgrading. These metals include gallium [33], lanthanum [34], copper alloys [35], [36], and nickel [37].

Cheng et al. synthesized a bifunctional Ga/ZSM-5 catalyst that was able to successfully convert furan into aromatic compounds. Gallium performed decarbonylation and aromatization reactions while the zeolite was responsible for oligomerization and cracking reactions. Reaction conditions were at 600°C, weight hourly space velocity (WHSV) at 10.4 hr⁻¹ with a furan partial pressure of 6 Torr. Their results suggest that, for aromatization to occur with light olefinic compounds, strong acidic sites are necessary. Although furan is not likely to be found in lignin, the reaction pathways of this catalyst may be interesting to explore for α -carbonyl groups typically found in natural lignin structure.

Zhao et al. reported an economical catalyst that was able to upgrade pyrolysis bio-oil from pine trees very efficiently. Nickel coupled with HZSM-5 catalysts showed a remarkable ability to catalyze both deoxygenation and hydrogenation reactions of phenolic compounds and bulky phenolic dimers present in bio-oil. Reaction conditions for these experiments took place at 250°C with 725 psi of H₂ under the presence of water (80 mL) for 2 hours [37]. The catalyst used in this reaction was prepared with 20 wt.% Ni coupled with HZSM-5 with a 45 Si/Al ratio, with average Ni particle size of 24 nm located inside the zeolite pores. High conversion of methoxylated phenolics with alkenyl functional groups were observed, with a large percentage of alkylated cyclohexanes and aromatics formed through the use of Ni/HZSM-5. These results differ greatly with the eugenol work done by Nimmanwudipong et al. [8] in which only partial

hydrogenation of the bulky alkenyl group was observed, resulting in 4-propylguaiacol. Although the two experiments differed greatly in their reaction conditions, it is worth noting that these results could be attributed to H₂ partial pressures used in each experiment (725 psi versus 20 psi). This is consistent with the previous observation that HDO reactions were strongly dependent on H₂ partial pressure [28]. Their results with both phenolic monomers and dimers are shown in Figure 2-7.

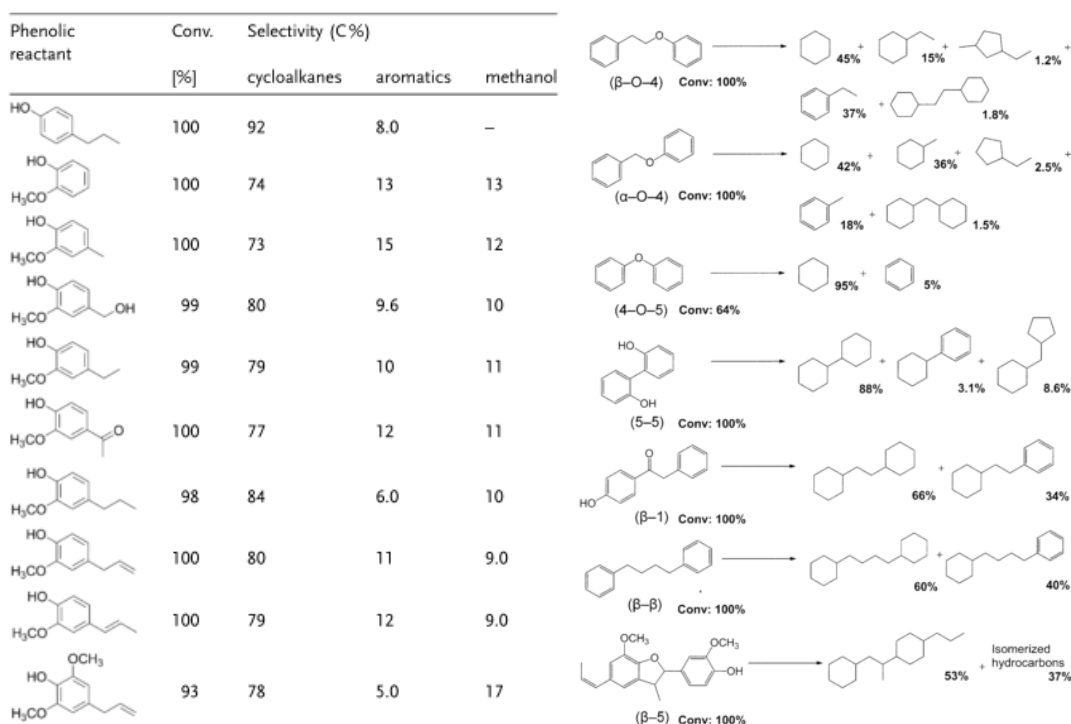


Figure 2-7. Hydrodeoxygenation of phenolic monomers and dimers with Ni/HZSM-5

Similarly, this "bulkiness" factor mentioned prior with alkenyl groups on eugenol is further evident with phenolic dimers bonded through α -O-4, β -O-4, 4-O-5, 5-5, β -1, β - β , and β -5 linkages, shown in Figure 2-8.

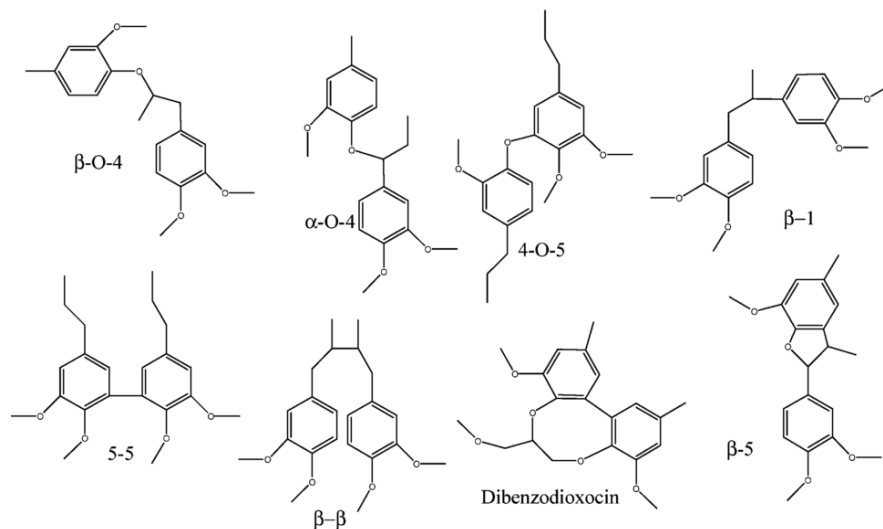


Figure 2-8. Common lignin linkages inherent in natural lignin

Ni/HZSM-5 catalyst bifunctionally catalyzed each of these linkages into gasoline-like chemicals that can be directly blended with existing gasoline [37]. More specifically, C-O-C linkages resulted in 98% conversion of C₆ and C₇ hydrocarbons. The authors hypothesized that the reaction route of these dimers followed a reaction network of hydrogenolysis of C-O bonds, followed with hydrogenation and dehydration reactions. Difficult 4-O-5 linkages were cleaved through C-O bond cleavage, representing the bifunctional catalytic effect to break aryl ether bonds. C-C bonds were preserved in the latter linkages, with oxygen-containing functional groups cleaved to produce C₁₂, C₁₄, and C₁₆ hydrocarbons as major products [37]. As mentioned previously, this conversion of sterically bulky functional groups may be the result of higher H₂ partial pressure and higher metal loading, resulting in improved hydrogenation performance. Through catalytic upgrading with Ni/HZSM-5, lignin compounds were deoxygenated and hydrogenated into molecules with higher octane numbers, as indicated in Figure 2-9 [37]. Lastly, Ni/HZSM-5 was able to sustain high catalytic stability, with no major differences in activity and selectivity over five cycles [37].


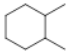
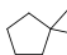

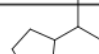
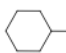
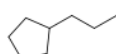
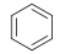
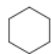
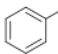
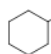
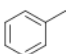
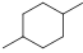
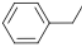
Hydro-carbon	Octane number (RON)	Hydro-carbon	Octane number (RON)
	101		81
	92		67
	81		63
	31		106
	83		120
	75		>100
	68		>100

Figure 2-9. Octane numbers for common cycloalkane and aromatic compounds

2.10 Bifunctional catalysis: Other metals supported on traditional supports

Platinum group metals are excellent catalysts as they are able to catalyze a multitude of reactions at milder temperatures and pressures. However, the demand and price for these metals puts them at an economic disadvantage. Other catalysts, such as nickel (Ni), cobalt (Co) [38], iron (Fe) [39], and copper (Cu) [40] are much cheaper and are capable catalysts. This section focuses on relevant literature on their applications with model compounds.

Mochizuki et al. examined the HDO of simulated bio-oil with guaiacol and real woody tar bio-oil over reduced Ni/SiO₂, Co/SiO₂, Pt/SiO₂, Pd/SiO₂, and sulfided CoMo/Al₂O₃ catalysts. Their experiments are meant for downstream upgrading of liquid bio-oil. Reactions were carried out from 1-5 MPa of H₂ with temperatures of 300-350°C in a batch reactor with

holding times of 1-3 hours. Out of the four catalysts tested, reduced Co/SiO₂ (20 wt.% Co) was the most effective in performing HDO reactions for both the simulated and real bio-oil, successfully deoxygenating 5 wt.% guaiacol into benzene and cyclohexane with an overall 100% conversion/96.4% HDO and 40% and 53% selectivity for both products respectively [38]. The authors also varied guaiacol content from 5% to 20% and noticed a steady decline in conversion, but no significant variation in selectivity. It is hypothesized that the Co/SiO₂ catalyst operates on guaiacol through a demethylation reaction to form catechol, which is subsequently dehydrated to phenol. Phenol is then directly deoxygenated (DDO) into benzene and hydrogenated to form cyclohexane. This reaction scheme is shown in Figure 2-10. Sulfided CoMo/Al₂O₃ performed hydrogenation reactions, noted as HYD, to form cyclohexanones instead.

The DDO reaction mechanism was hypothesized to occur as follows: weakly acidic silica sites bind directly to oxygen atoms on the hydroxyl and methoxyl bonds, while adsorbed hydrogen on the metal (Co) "spill-over" to complete the DDO reaction [38]. This scheme is shown in Figure 2-11. The authors also state that higher acidity is a major contributing factor to coke deposition, and that the low acidity from silica lowered coke deposition.

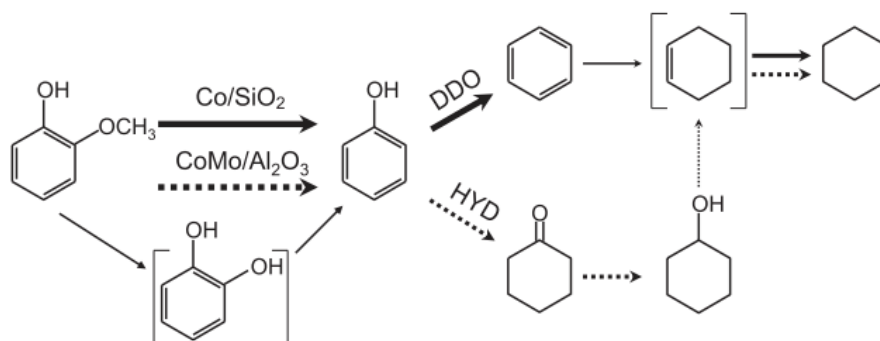


Figure 2-10. Reaction mechanism of guaiacol conversion into benzene over Co/SiO₂ compared to CoMo/Al₂O₃

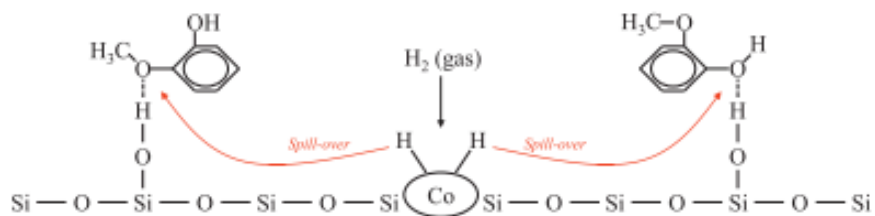


Figure 2-11. Guaiacol adsorption/reaction scheme predicted by Mochizuki et al.

Strassberger et al. tested copper/ γ - Al_2O_3 catalysts to catalyze model lignin dimers connected through β -O-4 linkages. It was observed that copper catalyzed the scission of these linkages, forming phenols and ethylbenzenes as a result. They observed that larger agglomerates of copper induced higher HDO selectivity, while higher copper dispersion lowered HDO selectivity on magnesia/alumina supports. Reactions were conducted in stainless steel autoclaves at 150°C with an initial H_2 pressure of 25 bar for 21 hours. Their hypothesized reaction mechanism is shown below in Figure 2-12.

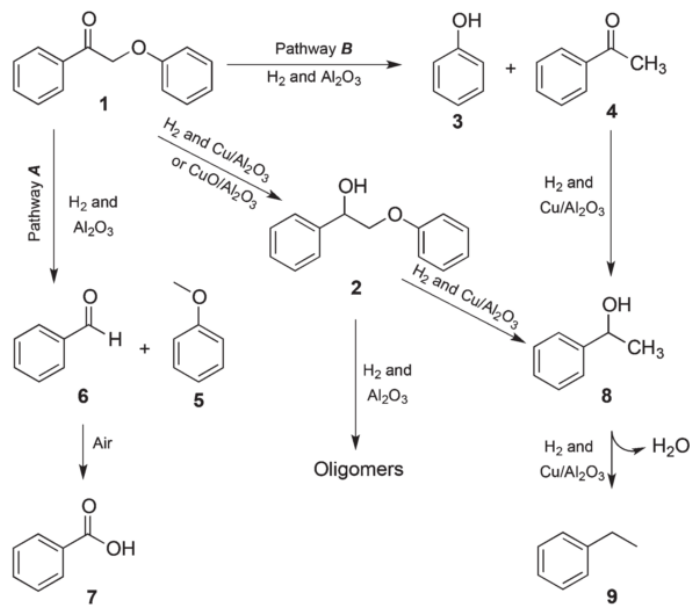


Figure 2-12. Reaction pathways of β -O-4 cleavage through copper supported on alumina

2.11 Summary

Hydrogenation and deoxygenation reactions are necessary to convert phenolic rings present in lignin pyrolysis into gasoline-range hydrocarbons. Lignin, through model compound studies and experimental thermal pyrolysis of biomass, has been studied using various bifunctional catalysts that show significant improvement over their monofunctional forms. Transition metals such as platinum, palladium, nickel, cobalt, among others were coupled with complementary supports such as zeolites, alumina, silica, and even carbon. The combination of these metals with a support often times demonstrated a synergistic catalytic effect that improved conversion, selectivity, and/or activation stability.

However, activation stability in high temperature, high pressure conditions, especially when working with high pressure hydrogen and bulky phenolic compounds, is especially important. Novel approaches in zeolite synthesis and nanoparticle production can contribute to improving mesoporosity and metal dispersion in the zeolites [14], [19]. Additionally, these improvements in bifunctional catalysis may allow for economical applications of expensive PGM nanocatalysts because of their efficient surface to volume ratio. It is also necessary to utilize other prevalent transition metals, alkali earth metals, and bimetallic alloys as potential new catalysts to further understand the catalytic pyrolysis of lignin.

It is important not to focus exclusively on model compounds to model the pyrolysis of natural lignin. The reaction pathways observed in model compounds such as phenol and guaiacol will vary considerably to the bulk heterostructure of natural lignin. As a result, further work that juxtaposes the analysis of model compounds with natural lignin will be far more insightful. As

this topic is in its infancy, there is much to be discovered in terms of efficient reactor design, tunable multifunctional catalysts, and the kinetic rate laws that govern these transformations.

2.12 References

- [1] D. A. Simonetti and J. A. Dumesic, “Catalytic strategies for changing the energy content and achieving C–C coupling in biomass-derived oxygenated hydrocarbons.,” *ChemSusChem*, vol. 1, pp. 725–33, Jan. 2008.
- [2] G. W. Huber, S. Iborra, and C. Avelino, “Synthesis of transportation fuels from biomass: chemistry, catalysts, and engineering,” *Chemical Reviews*, vol. 106, no. 9, pp. 4044–4098, 2006.
- [3] D. A. Bulushev and J. R. Ross, “Catalysis for conversion of biomass to fuels via pyrolysis and gasification: A review,” *Catalysis Today*, vol. 171, pp. 1–13, Aug. 2011.
- [4] “U.S. Climate Action Report,” *United States Department of State*, 2006.
- [5] T. Nimmanwudipong, “Catalytic Conversion of Lignin-Derived Compounds to Fuels and Chemicals,” *UC Davis*, 2012.
- [6] P. Azadi, O. R. Inderwildi, R. Farnood, and D. A. King, “Liquid fuels, hydrogen and chemicals from lignin: A critical review,” *Renewable and Sustainable Energy Reviews*, vol. 21, pp. 506–523, May 2013.
- [7] D. M. Alonso, S. G. Wettstein, and J. A. Dumesic, “Bimetallic catalysts for upgrading of biomass to fuels and chemicals.,” *Chemical Society reviews*, vol. 41, pp. 8075–98, Dec. 2012.
- [8] T. Nimmanwudipong, R. C. Runnebaum, S. E. Ebeler, D. E. Block, and B. C. Gates, “Upgrading of Lignin-Derived Compounds: Reactions of Eugenol Catalyzed by HY Zeolite and by Pt/ γ -Al₂O₃,” *Catalysis Letters*, vol. 142, pp. 151–160, Dec. 2011.
- [9] P. de Wild, R. V. D. Laan, K. Rug, and E. Heeres, “Lignin Valorisation for Chemicals and (Transportation) Fuels via (Catalytic) Pyrolysis and Hydrodeoxygenation,” *Environmental Progress & Sustainable Energy*, vol. 28, no. 3, pp. 461–469, 2009.
- [10] K. Jacobson, K. C. Maheria, and A. Kumar Dalai, “Bio-oil valorization: A review,” *Renewable and Sustainable Energy Reviews*, vol. 23, pp. 91–106, July 2013.
- [11] P. Mortensen, J. Grunwaldt, P. Jensen, K. Knudsen, and A. Jensen, “A review of catalytic upgrading of bio-oil to engine fuels,” *Applied Catalysis A: General*, vol. 407, pp. 1–19, Nov. 2011.
- [12] H. Kato, T. Minami, T. Kanazawa, and Y. Sasaki, “Mesopores created by platinum nanoparticles in zeolite crystals.,” *Angewandte Chemie (International ed. in English)*, vol. 43, pp. 1251–4, Feb. 2004.
- [13] X. Zhu, R. G. Mallinson, and D. E. Resasco, “Role of transalkylation reactions in the conversion of anisole over HZSM-5,” *Applied Catalysis A: General*, vol. 379, pp. 172–181,

May 2010.

- [14] X. Zhu, L. L. Lobban, R. G. Mallinson, and D. E. Resasco, "Bifunctional transalkylation and hydrodeoxygenation of anisole over a Pt/HBeta catalyst," *Journal of Catalysis*, vol. 281, pp. 21–29, July 2011.
- [15] Q. Lu, Z. Tang, Y. Zhang, and X. F. Zhu, "Catalytic Upgrading of Biomass Fast Pyrolysis Vapors with Pd/SBA-15 Catalysts," *Industrial & Engineering Chemistry Research*, vol. 49, pp. 2573–2580, Mar. 2010.
- [16] P. Barbaro, F. Liguori, N. Linares, and C. M. Marrodan, "Heterogeneous Bifunctional Metal/Acid Catalysts for Selective Chemical Processes," *European Journal of Inorganic Chemistry*, vol. 2012, pp. 3807–3823, Aug. 2012.
- [17] K. O. Albrecht, "A Brief Literature Overview of Various Routes to Biorenewable Fuels from Lipids for the National Alliance for Advanced Biofuels and Bio-products (NAABB) Consortium," no. March, 2011.
- [18] I. Chorkendorff and J. Niemantsverdriet, *Concepts of Modern Catalysis and Kinetics*. 2007.
- [19] M. Zahmakran and S. Ozkar, "Metal nanoparticles in liquid phase catalysis; from recent advances to future goals," *Nanoscale*, vol. 3, pp. 3462–81, Sept. 2011.
- [20] N. Yan and P. J. Dyson, "Transformation of biomass via the selective hydrogenolysis of CO bonds by nanoscale metal catalysts," *Current Opinion in Chemical Engineering*, vol. 2, pp. 178–183, May 2013.
- [21] W. Yu, Y. Tang, L. Mo, P. Chen, H. Lou, and X. Zheng, "One-step hydrogenation-esterification of furfural and acetic acid over bifunctional Pd catalysts for bio-oil upgrading," *Bioresource technology*, vol. 102, pp. 8241–6, Sept. 2011.
- [22] P. Treesukol, K. Srisuk, J. Limtrakul, and T. N. Truong, "Nature of the metal-support interaction in bifunctional catalytic Pt/H-ZSM-5 zeolite," *Journal of Physical Chemistry B*, vol. 109, pp. 11940–5, June 2005.
- [23] H. Wang, J. Male, and Y. Wang, "Recent Advances in Hydrotreating of Pyrolysis Bio-Oil and Its Oxygen-Containing Model Compounds," *ACS Catalysis*, vol. 3, pp. 1047–1070, May 2013.
- [24] D.-Y. Hong, S. J. Miller, P. K. Agrawal, and C. W. Jones, "Hydrodeoxygenation and coupling of aqueous phenolics over bifunctional zeolite-supported metal catalysts," *Chemical communications (Cambridge, England)*, vol. 46, pp. 1038–40, Feb. 2010.
- [25] J. Horacek, G. Šávková, V. Kelbichová, and D. Kubic̃ka, "Zeolite-Beta-supported platinum catalysts for hydrogenation/hydrodeoxygenation of pyrolysis oil model compounds," *Catalysis Today*, vol. 204, pp. 38–45, Apr. 2013.
- [26] A. Corma, A. Mart, and V. Mart, "Hydrogenation of Aromatics in Diesel Fuels on Pt /

- MCM-41 Catalysts,” *Journal of Catalysis*, vol. 489, pp. 480–489, 1997.
- [27] C. R. Lee, J. S. Yoon, Y.-W. Suh, J.-W. Choi, J.-M. Ha, D. J. Suh, and Y.-K. Park, “Catalytic roles of metals and supports on hydrodeoxygenation of lignin monomer guaiacol,” *Catalysis Communications*, vol. 17, pp. 54–58, Jan. 2012.
- [28] T. Nimmanwudipong, R. C. Runnebaum, D. E. Block, and B. C. Gates, “Catalytic Conversion of Guaiacol Catalyzed by Platinum Supported on Alumina: Reaction Network Including Hydrodeoxygenation Reactions,” *Energy & Fuels*, vol. 25, pp. 3417–3427, Aug. 2011.
- [29] R. C. Runnebaum, T. Nimmanwudipong, D.E. Block, and B. C. Gates, “Catalytic conversion of compounds representative of lignin-derived bio-oils: a reaction network for guaiacol, anisole, 4-methylanisole, and cyclohexanone conversion catalysed by Pt/ γ -Al₂O₃,” *Catalysis Science & Technology*, vol. 2, no. 1, p. 113, 2012.
- [30] X. Xu, Y. Li, Y. Gong, P. Zhang, H. Li, and Y. Wang, “Synthesis of Palladium Nanoparticles Supported on Mesoporous N-Doped Carbon and Their Catalytic Ability for Biofuel Upgrade,” *Journal of the American Chemical Society*, no. 134, pp. 16987–16990, 2012.
- [31] C. Zhao, W. Song, and J. A. Lercher, “Aqueous Phase Hydroalkylation and Hydrodeoxygenation of Phenol by Dual Functional Catalysts Comprised of Pd/C and H/La-BEA,” *ACS Catalysis*, vol. 2, pp. 2714–2723, Dec. 2012.
- [32] S. Crossley, J. Faria, M. Shen, and D. E. Resasco, “Solid nanoparticles that catalyze biofuel upgrade reactions at the water/oil interface,” *Science (New York, N.Y.)*, vol. 327, pp. 68–72, Jan. 2010.
- [33] Y.T. Cheng, J. Jae, J. Shi, W. Fan, and G. W. Huber, “Production of renewable aromatic compounds by catalytic fast pyrolysis of lignocellulosic biomass with bifunctional Ga/ZSM-5 catalysts,” *Angewandte Chemie (International ed. in English)*, vol. 51, pp. 1387–90, Feb. 2012.
- [34] W. Huang, F. Gong, M. Fan, Q. Zhai, C. Hong, and Q. Li, “Production of light olefins by catalytic conversion of lignocellulosic biomass with HZSM-5 zeolite impregnated with 6wt.% lanthanum,” *Bioresource technology*, vol. 121, pp. 248–55, Oct. 2012.
- [35] P. Sai Prasad, J. W. Bae, S.-H. Kang, Y.-J. Lee, and K.-W. Jun, “Single-step synthesis of DME from syngas on CuZnOAl₂O₃/zeolite bifunctional catalysts: The superiority of ferrierite over the other zeolites,” *Fuel Processing Technology*, vol. 89, pp. 1281–1286, Dec. 2008.
- [36] T. T. Pham, L. L. Lobban, D. E. Resasco, and R. G. Mallinson, “Hydrogenation and Hydrodeoxygenation of 2-methyl-2-pentenal on supported metal catalysts,” *Journal of Catalysis*, vol. 266, pp. 9–14, Aug. 2009.
- [37] C. Zhao and J. A. Lercher, “Upgrading pyrolysis oil over Ni/HZSM-5 by cascade

reactions.,” *Angewandte Chemie (International ed. in English)*, vol. 51, pp. 5935–40, June 2012.

- [38] T. Mochizuki, S.Y. Chen, M. Toba, and Y. Yoshimura, “Deoxygenation of Guaiacol and Woody Tar over Reduced Catalysts,” *Applied Catalysis B: Environmental*, May 2013.
- [39] R. Olcese, M. Bettahar, B. Malaman, J. Ghanbaja, L. Tibavizco, D. Petitjean, and A. Dufour, “Gas-phase hydrodeoxygenation of guaiacol over iron-based catalysts. Effect of gases composition, iron load and supports (silica and activated carbon),” *Applied Catalysis B: Environmental*, vol. 129, pp. 528–538, Jan. 2013.
- [40] Z. Strassberger, A. H. Alberts, M. J. Louwerse, S. Tanase, and G. Rothenberg, “Catalytic cleavage of lignin β -O-4 link mimics using copper on alumina and magnesiaalumina,” *Green Chemistry*, vol. 15, no. 3, p. 768, 2013.

CHAPTER 3 MATERIALS AND EXPERIMENTAL METHODS

3.1 Lignin

Lignin used throughout this study was prepared via sulfur catalyzed steam explosion of hybrid poplar (195°C, 3% SO₂, 5 minutes). Klason acid hydrolysis (121°C, 72% H₂SO₄, 60 minutes) was performed to further purify the poplar lignin of any residues and undissolved sugars.

3.2 Catalyst preparation

ZSM-5 (CBV-2314, Zeolyst International) was purchased in the nominal ammonium cation form. The acidic form, HZSM-5, was prepared by calcination in air for 5 hours at 600°C. The specified surface area was 425 m²/g with a SiO₂/Al₂O₃ ratio of 23.

Pd/HZSM-5 catalysts were prepared through an incipient wetness impregnation technique. An appropriate amount of Pd(NO₃)₂·6H₂O and HZSM-5 were mixed to obtain 1 wt.% loading of Pd with respect to the total catalyst at 700 rpm in deionized water at room temperature for 24 hrs. The water was then removed via evaporation. The resulting dried catalyst was calcined at 600°C for 2 hours under oxygen gas. Finally, the catalyst was reduced in 10% H₂, 90% argon gas at 550°C for 3 hours.

3.3 *Hydropyrolysis-gas chromatography/mass spectrometry*

Microscale hydropyrolysis experiments were conducted using a Pyroprobe 5200 model with high pressure and reactant gas options (Chemical Data Systems Analytical). The pyroprobe system was equipped with a platinum coil that served simultaneously as a sample holder and resistive heating element. Hydropyrolysis samples were prepared in quartz tubes with up to 0.5 mg of lignin and/or catalyst surrounded by two layers of quartz wool, as described previously.⁴ An analytical balance with a resolution of 0.1 μg was used for accurate weighing of hydropyrolysis samples (AD 6000 Ultra Microbalance, Perkin Elmer). Catalysts were mixed with lignin in ratios of 1:1, 10:1, and 20:1 in in-situ experiments. Fresh catalysts were used for all trials. A simplified process flow diagram (PFD) of the pyroprobe operated with the ex-situ reactor is shown below in Figure 3-1, where the catalyst is in section B in between two layers of quartz wool. For in-situ experiments, there was no catalyst in section B. The reactor was approximately 141°C for all in-situ experiments.

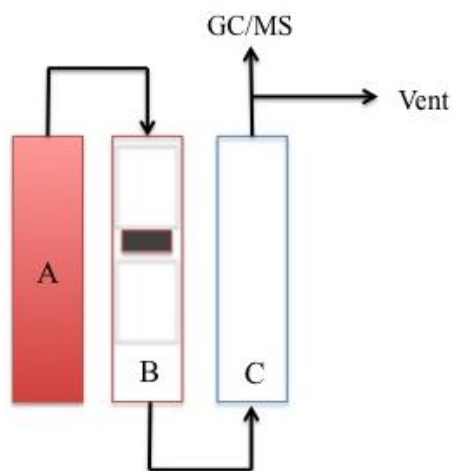


Figure 3-1. Pyroprobe PFD. A: Pyroprobe, B: Packed bed reactor, C: In-line trap

The pressure in the pyroprobe unit was controlled using a high-pressure module. A backpressure regulator maintained the pressure within the system. 6.0-grade helium gas (99.9999%) acted as the carrier/sweeping gas. The valve oven and transfer line were both set constant at 300°C throughout all experiments. 5.0-grade H₂ reactant gas (99.999%) was introduced during the interface temperature ramp. The initial interface temperature was set to 100°C and it ramped to 300°C upon software initialization. Once the interface temperature was stable at 300°C, the platinum coil rapidly heated to the set point at a ramp of 1000°C/s and the set point temperature was maintained for 60 seconds. Vapors produced from hydrolysis were then absorbed onto a downstream TENAX trap at 50°C to allow for pyrolysate collection. However, permanent gases could not be collected by this trapping setup and were sent through the purge vent. Upon completion, hydrolysis products absorbed onto the trap were then thermally desorbed at 300°C for 5 minutes and swept by helium into a gas chromatography/mass spectrometer system for downstream analysis (QP2010 Ultra, Shimadzu).

The Pyroprobe 5200 also has a downstream packed bed reactor that can be used for ex-situ catalytic upgrading. This reactor is labeled as B in Figure 1 and is loaded with a layer of catalyst surrounded by two plugs of quartz wool. The temperature of the packed bed reactor is controlled using the high-pressure module and has a maximum temperature reading of 800°C. The temperature reader is located on the exterior of the reactor so this temperature reading corresponds to the outer wall temperature instead of the temperature inside the reactor. The TENAX trap further downstream will absorb the product stream coming out of the reactor before being analyzed.

Gas chromatography/mass spectrometry (GC/MS) was used to qualitatively and quantitatively determine the volatile hydrolysis products. The injector was kept at a constant

300°C. Chromatographic separation of the hydropyrolysis products was achieved using a ZB-5ms capillary column (30m length x 0.25mm inner diameter x 0.25 μ m film thickness) (Phenomenex). The helium flow rate was set to 206.5 mL/min at an initial pressure of 113.3 kPa, and a split ratio of 125. The temperature of the GC oven started at 35°C (held for 2 minutes), followed by a ramp to 200°C at 5°C/min (held at 200°C for 5 minutes), and ramped to 300°C at 10°C/min (held for 5 minutes). The mass spectrometer was operated at 0.88 kV in SCAN mode. Target masses were analyzed from m/z of 45.00 to 500.00 at a scan speed of 1666 amu/s. NIST MS libraries were used to identify chromatographic peaks of compounds with a similarity index of 90 or greater.

In this work, we report only the volatile products at 300°C. There are also permanent gases (CO, CO₂, CH₄) and non-volatile compounds that could not be measured with the pyroprobe setup. In addition, the mass of the resulting solid (catalyst+coke) was too small to be measured accurately and is not reported.

3.4 *Elemental Analysis*

An elemental analyzer (EA 2400, Perkin Elmer) was used to determine the weight percentages of carbon, hydrogen, and nitrogen. An analytical balance with a resolution of 0.1 μ g was used for accurate weighing of samples and k-factors.

3.5 *Data analysis*

Five point calibration curves of major hydropyrolysis products (similarity index > 90) were constructed using analytical standards purchased from Sigma Aldrich and Fisher through autosampler injection in HPLC-grade methanol. 50 compounds were quantified by TIC using 19

external standards: 7 aromatic hydrocarbons and 12 phenolics as specified in Table 3-1. Response factors for the remaining compounds were approximated by those of standards with similar chemical structures. All trials were performed in triplicates for reproducibility. Error bars reported represent the standard deviations of the replicated trials.

No.	Compound	R.T.	Formula	M.M.	Family	Quantification
1	1,3-Cyclopentene	2.624	C ₅ H ₈	68.11	Cycloalkene	Benzene
2	Cyclopentane, methyl-	3.361	C ₆ H ₁₂	84.16	Cycloalkane	Toluene
3	Benzene	3.858	C ₆ H ₆	78.11	Aromatic	Standard
4	Cyclopentane, 1,3-dimethyl	4.152	C ₇ H ₁₄	98.19	Cycloalkane	Xylene
5	Cyclohexane, methyl-	4.875	C ₇ H ₁₄	98.19	Cycloalkane	Toluene
6	Toluene	5.97	C ₇ H ₈	92.14	Aromatic	Standard
7	Cyclohexane, 1,4-dimethyl-	6.189	C ₈ H ₁₆	112.21	Cycloalkane	Xylene
8	Cyclohexane, ethyl-	7.705	C ₈ H ₁₆	112.21	Cycloalkane	Ethylbenzene
9	Ethylbenzene	8.643	C ₈ H ₁₀	106.17	Aromatic	Standard
10	m-Xylene	8.813	C ₈ H ₁₀	106.16	Aromatic	Standard
11	p-Xylene	8.888	C ₈ H ₁₀	106.16	Aromatic	Standard
12	o-Xylene	9.538	C ₈ H ₁₀	106.16	Aromatic	Standard
13	Styrene	9.541	C ₈ H ₈	104.15	Aromatic	p-xylene
14	Ethylmethylbenzene	11.847	C ₉ H ₁₂	120.19	Aromatic	Standard
15	Phenol	12.445	C ₆ H ₆ O	94.11	Phenolic	Standard
16	Trimethylbenzene	12.817	C ₉ H ₁₂	120.19	Aromatic	Standard
17	Benzofuran	12.915	C ₈ H ₆ O	118.13	Phenolic	Toluene
18	Indane	14.161	C ₉ H ₁₀	118.18	Cycloalkene	Benzene
19	2-Hydroxybenzaldehyde	14.381	C ₇ H ₆ O ₂	122.12	Phenolic	Vanillin
20	Indene	14.432	C ₉ H ₈	116.16	Cycloalkene	Ethylbenzene
21	m-Cresol	14.432	C ₇ H ₈ O	108.13	Phenolic	2,4-xylenol

22	p-Cresol	14.739	C ₇ H ₈ O	108.13	Phenolic	2,4-xylenol
23	Guaiacol	15.834	C ₇ H ₈ O ₂	124	Phenolic	Standard
24	2,3-Xylenol	16.351	C ₈ H ₁₀ O	122	Phenolic	2,4-xylenol
25	Methylbenzofuran	16.434	C ₉ H ₈ O	132	Phenolic	Toluene
26	Ethylphenol	17.3	C ₈ H ₁₀ O	122	Phenolic	2,4-xylenol
27	2,3-Dihydro-4-methylindene	17.373	C ₁₀ H ₁₂	132	Cycloalkene	Ethylbenzene
28	Methylpropenylbenzene	17.38	C ₁₂ H ₁₂	132	Aromatic	Ethylbenzene
29	2,5-Xylenol	17.597	C ₈ H ₁₀ O	122	Phenolic	2,4-xylenol
30	Methylindene	17.846	C ₁₀ H ₁₀	130.2	Cycloalkene	Toluene
31	Xylenol	18.207	C ₈ H ₁₀ O	122	Phenolic	2,4-xylenol
32	2-Methoxy-3-methylphenol	18.543	C ₈ H ₁₀ O ₂	138	Phenolic	Creosol
33	Naphthalene	18.723	C ₁₀ H ₈	128.2	Aromatic	Toluene
34	Creosol	18.969	C ₈ H ₁₀ O ₂	138	Phenolic	Standard
35	Catechol	19.066	C ₆ H ₆ O ₂	110.1	Phenolic	Standard
36	Trimethylphenol	19.255	C ₉ H ₁₂ O	136.19	Phenolic	2,4-xylenol
37	4-Methylcatechol	20.857	C ₇ H ₈ O ₂	124	Phenolic	Standard
38	Ethylmethoxyphenol	20.943	C ₉ H ₁₂ O ₂	152.2	Phenolic	Ethylguaiacol
39	4-Ethyl-2-methoxyphenol	21.424	C ₉ H ₁₂ O ₂	152.2	Phenolic	4-ethylguaiacol
40	Methylcatechol	21.656	C ₇ H ₈ O ₂	124	Phenolic	4-methylcatechol
41	Methylnaphthalene	21.889	C ₁₁ H ₁₀	142.2	Aromatic	Toluene
42	2-Methoxy-4-vinylphenol	22.388	C ₉ H ₁₀ O ₂	150	Phenolic	Standard
43	3-Methoxy-5-methylphenol	22.504	C ₈ H ₁₀ O ₂	138	Phenolic	Creosol
44	p-Eugenol	23.561	C ₁₀ H ₁₂ O ₂	164	Phenolic	Standard
45	2-Methoxy-4-propylphenol	23.824	C ₁₀ H ₁₄ O ₂	166	Phenolic	Standard
46	4-Ethylcatechol	24.178	C ₈ H ₁₀ O ₂	138	Phenolic	Standard
47	Vanillin	24.644	C ₈ H ₈ O ₃	152	Phenolic	Standard

48	Apocynin	26.855	C ₉ H ₁₀ O ₃	166	Phenolic	Standard
59	Fluorene	29.243	C ₁₃ H ₁₀	166.22	Aromatic	Toluene
50	Phenanthrene	33.861	C ₁₄ H ₁₀	178.23	Aromatic	Toluene

Table 3-1. Hydropyrolysis products with and without catalysts

CHAPTER 4 RESULTS AND DISCUSSION

Throughout this work, yield is defined as

$$\%yield_i = \frac{\text{mass of compound } i \text{ in product}}{\text{mass of lignin}} \times 100$$

as used previously [1], [2].

4.1 Lignin characterization

The elemental composition of the steam exploded poplar lignin was determined on a CHNS/O Elemental Analyzer (EA 2400, Perkin Elmer). The results are shown in Table 4-1.

C(%)	H (%)	N (%)	O (%) (by difference)	S (%)*
61.7 ± 0.1	3.21 ± 1.02	0.267 ± 0.025	34.5 ± 1.0	0.24

Table 4-1. Elemental analysis of poplar lignin, *=tested by ICP/OES, single run

4.2 Noncatalytic hydrolysis of lignin

Poplar lignin was first pyrolyzed in H₂ in the absence of catalysts to determine the base case product distribution, as shown in Figure 4-1. Phenols (phenol, m/p cresol, catechol, methylcatechol), guaiacols (guaiacol, creosol), and syringol were amongst the most prevalent phenolic compounds observed and are listed in Figure 4-1. Trace amounts of aromatic compounds were detected during this initial study.

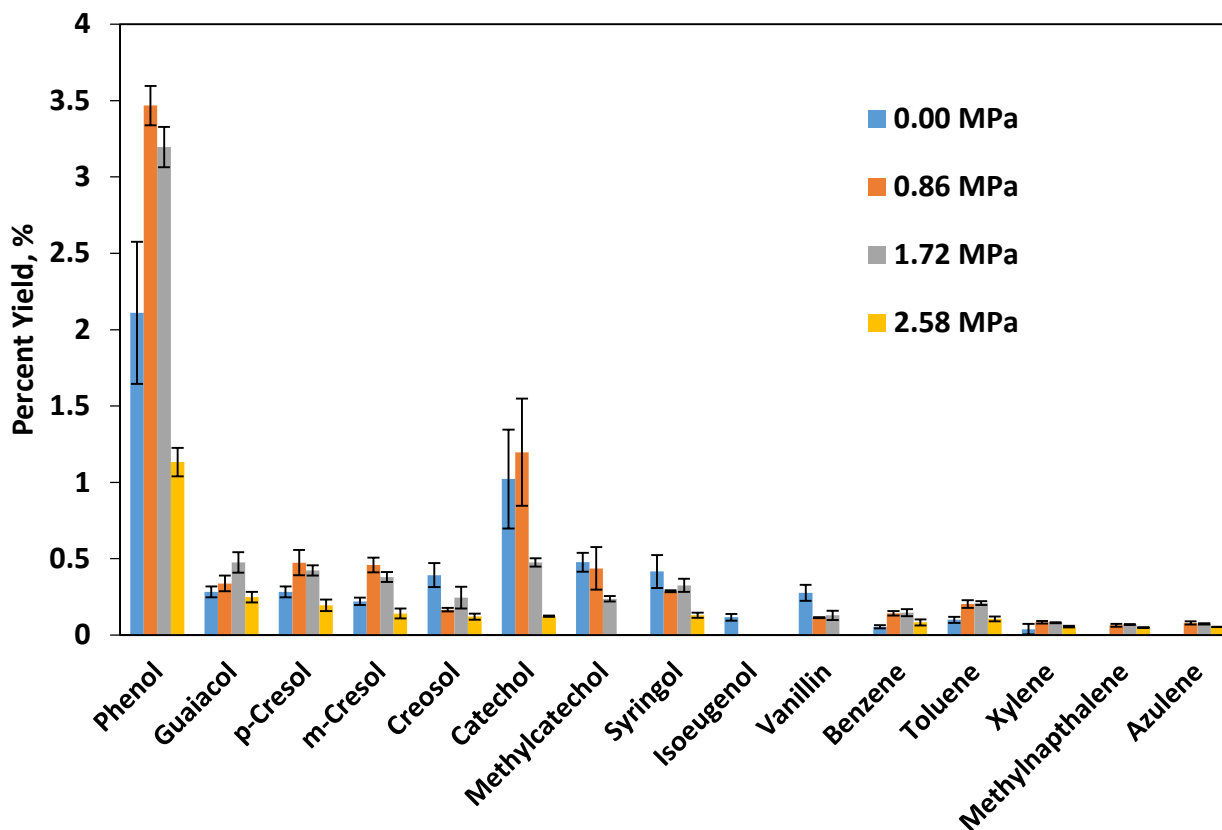


Figure 4-1. Major phenolic and aromatic products produced from noncatalytic hydrolysis of lignin at 650°C

We increased the H_2 partial pressure (gauge) to determine its effect on noncatalytic hydrolysis of lignin. For major compounds such as guaiacol and m/p cresol, the overall effect of H_2 partial pressure was small from 0.00 to 1.72 MPa. However, smaller yields of larger oxygenated compounds (catechol, methylcatechol, isoeugenol, vanillin) were observed at higher pressures. Conversely, as the H_2 partial pressure increased, there was an apparent increase in the yields of the aforementioned aromatic compounds (benzene, toluene, xylenes, methylnaphthalene, azulene). Interestingly, phenol yields increased from about 2 wt.% to approximately 3.5 wt.% as the H_2 partial pressure increased from 0.00 MPa to 0.85 MPa. Overall, the results suggest that H_2 , in the absence of catalysts, has only a minor role in deoxygenating larger phenolic compounds into phenol, with further deoxygenation into aromatic hydrocarbons.

H₂, particularly at high temperatures, may induce hydrogenolysis mechanisms where H₂ radicals promote demethoxylation, decarbonylation, and dehydration reactions.

Interestingly, the yields of all aromatic and phenolic compounds decreased as the H₂ partial pressure was further increased to 2.58 MPa. This suggests that a pressurized H₂ environment may induce severe hydrogenolysis of the lignin structure and increased production of noncondensable gases i.e., CO, CO₂, CH₄, C₂H₄, C₂H₆. The highly acidic pretreatment process may have resulted in a structurally weaker lignin as mentioned previously, making it more susceptible to hydrogenolysis by H₂ radicals. However, the yields of noncondensable gases could not be quantified by GC/MS due to experimental limitations of the hydrolysis system, so this hypothesis could not be confirmed.

4.3 Catalytic hydrolysis of lignin

Catalytic hydrolysis of lignin was studied using HZSM-5 and Pd/HZSM-5 catalysts mixed with lignin in the pyroprobe. The catalyst-to-lignin ratio, H₂ partial pressure, and hydrolysis temperature were varied in this study to observe their effect on the yields of aromatic hydrocarbons and cycloalkanes.

4.3.1. Effect of catalyst-to-lignin ratio

This study aimed to determine the optimal amount of catalyst necessary to generate a high aromatic hydrocarbon yield and low phenolic yield for HZSM-5 and Pd/HZSM-5 catalysts. For each catalyst, three catalyst-to-lignin ratios were used: 1:1, 10:1, and 20:1. It has been previously observed that higher ratios of catalyst to biomass have a positive effect on the hydrocarbon yield [3]. We performed screening experiments in the pressure range of 0.00-2.58 MPa at 650°C.

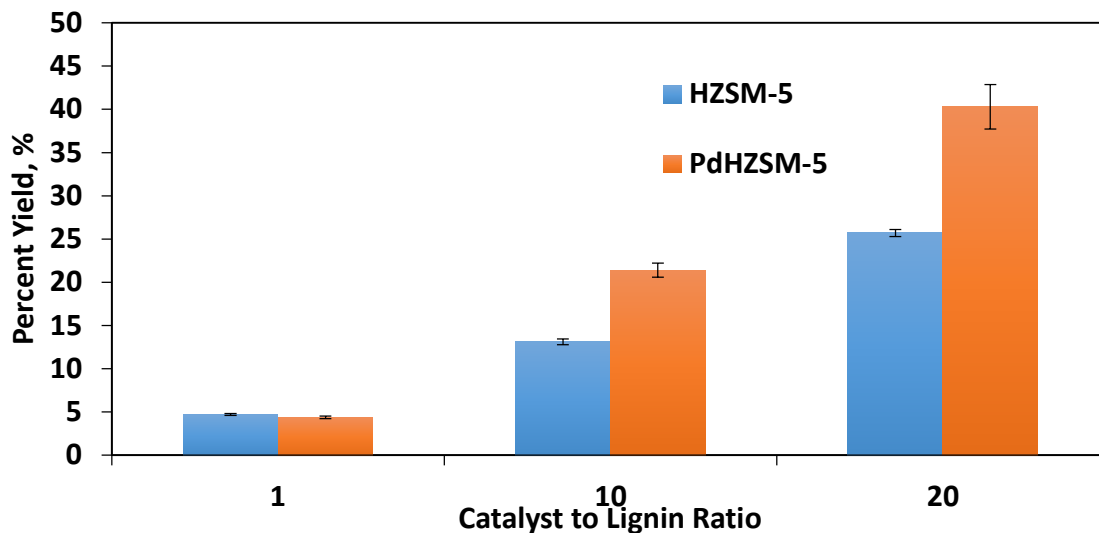


Figure 4-2. Effect of palladium on total aromatic hydrocarbon yield. Reaction conditions: $T_{\text{pyr}}=650^{\circ}\text{C}$, $P_{\text{H}}=1.72$ MPa

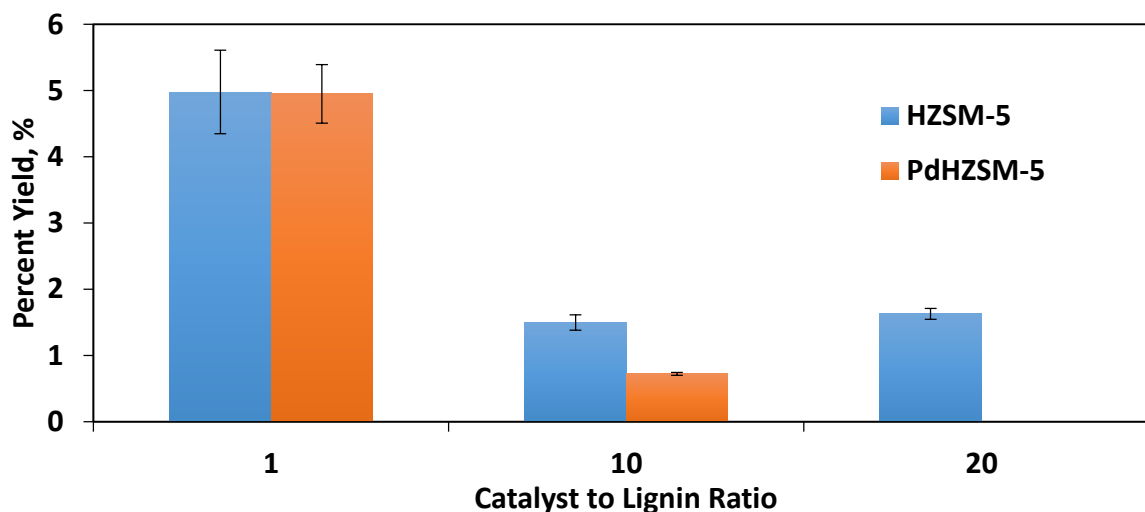


Figure 4-3. Effect of palladium on phenolic yield. Reaction conditions: $T_{\text{pyr}}=650^{\circ}\text{C}$, $P_{\text{H}}=1.72$ MPa

Within the range studied, the optimal experimental conditions for aromatic hydrocarbon generation and deoxygenation occurred at a H_2 partial pressure of 1.72 MPa. Only this situation is reported in Figures 4-2 and 4-3. At the lowest catalyst-to-lignin ratio (1:1), Pd/HZSM-5 catalyst behaves similarly to HZSM-5, as both catalysts produce similar yields of aromatic hydrocarbons as shown in Figure 4-2. In Figure 4-3, both catalysts produced a similar amount of

phenolic compounds with no major statistical differences in their deoxygenation ability. However, as the catalyst-to-lignin ratio increased from 1:1 to 10:1 to 20:1, Pd/HZSM-5 surpassed HZSM-5 at each ratio in aromatic hydrocarbon yield and phenolic deoxygenation.

At a 20:1 catalyst-to-lignin ratio, Pd/HZSM-5 produced 44% more aromatic hydrocarbons than HZSM-5 alone and virtually no phenolic compounds were detected through mass spectrometry with Pd/HZSM-5. These results suggest that the Pd metal is capable of accelerating deoxygenation and aromatization reactions that are normally facilitated by HZSM-5, resulting in higher yields of aromatic hydrocarbons. However, throughout these experiments, no cycloalkanes were observed. This indicates that hydrogenation is not a major reaction pathway at these conditions. Similarly, Thangalazhy-Gopakumar et. al. observed no cycloalkane products using pinewood biomass with metal-supported zeolites at a hydrolysis temperature of 650°C. No cycloalkane formation was observed with Ni/HZSM-5, Co/HZSM-5, Mo/HZSM-5, and Pt/HZSM-5, with minimal variation in aromatic hydrocarbon yield over a range of operating pressures amongst the four catalysts [4]. As the catalytic effect of the additional Pd metal was more evident at a catalyst-to-lignin ratio of 20:1 and H₂ partial pressure of 1.72 MPa, all remaining experiments reported were performed at these conditions, unless mentioned otherwise.

To explain the effects of adding a metal to a support, various research groups have alluded to a synergistic effect that leads to an improvement in the overall catalytic performance [5]–[12]. The Resasco group looked at the effect of using Pt/HBeta with lignin model compound anisole. It was observed that Pt/HBeta catalyst was an effective catalyst in the hydrodeoxygenation of anisole to aromatic compounds. They hypothesized that the Pt metal accelerated alkyl transfer reactions while adjacent Bronsted acid sites were responsible for carrying out deoxygenation reactions [8]. Ga/HZSM-5 was investigated by Cheng et. al. for

improving the rate of aromatic production from lignocellulosic biomass. Cheng et. al. hypothesized catalytic bifunctionality in which Ga improved the rates of decarbonylation and olefin aromatization while the zeolite was responsible for oligomerization reactions, thereby leading to an improvement in aromatic yield over monofunctional zeolite [11]. We believe that this synergistic effect plays a substantial role with Pd/HZSM-5 and lignin during hydrolysis.

4.3.2. Effect of H₂ partial pressure

The effect of H₂ partial pressure was investigated at 0.00, 0.86, 1.72, and 2.58 MPa. It is hypothesized that the presence of H₂ plays a critical role in hydrodeoxygenation reactions by providing a source of hydrogen atoms for hydrogenation and hydrogenolysis reactions. Figure 4-4 shows the effect of H₂ partial pressure on the overall yields of aromatic hydrocarbons at a hydrolysis temperature of 650°C and a catalyst-to-lignin ratio of 20. Surprisingly, for Pd/HZSM-5, there was a 43% decrease in aromatic hydrocarbon yield as the H₂ partial pressure increased from 0.00 MPa to 0.86 MPa. At this point, the reasons for this trend are not clearly understood.

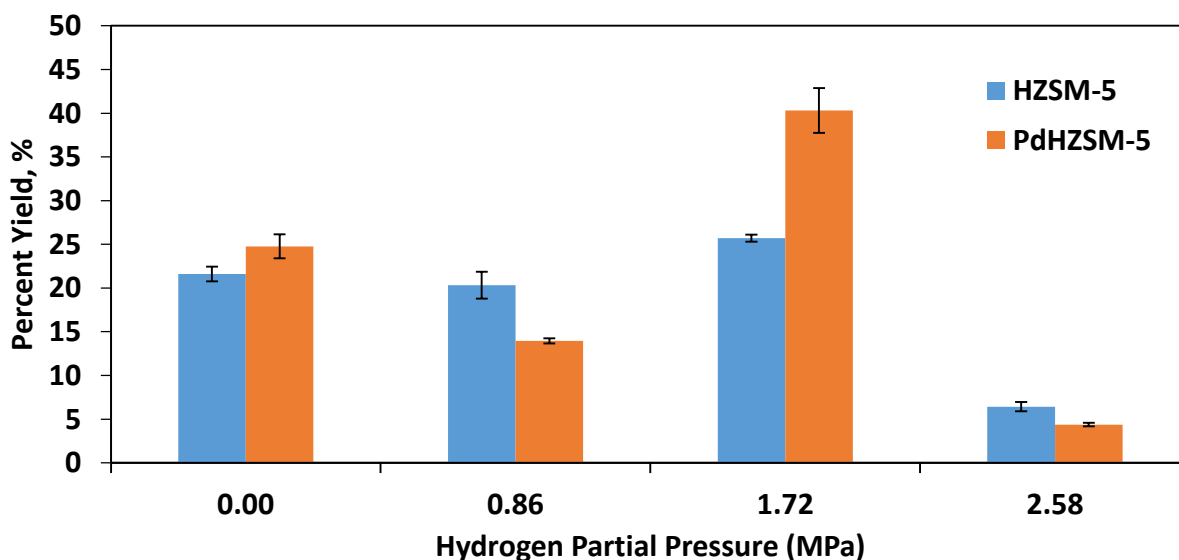


Figure 4-4. Effect of H₂ partial pressure on aromatic hydrocarbon for HZSM-5 and Pd/HZSM-5. T=650°C, catalyst-to-lignin ratio: 20

The optimal pressure for aromatic hydrocarbon formation within the range studied was observed at 1.72 MPa with an approximate aromatic yield of 40 wt.% with Pd/HZSM-5. This particular result indicates that a moderate partial pressure of H₂ positively impacts deoxygenation reactions performed by Pd/HZSM-5, with a noticeable 44% improvement over HZSM-5 (26 wt.%). Additionally, the maximum H₂ partial pressure tested (2.58 MPa) resulted in a severe decrease in aromatic yield for both catalysts. This is similar to the result mentioned in section 4.2 where we observed a marked decrease in overall yield. We suggest that the same hydrogenolysis mechanisms discussed previously causes this decrease in yield.

4.3.3 Effect of Pd on product distribution

Aromatic compounds, from C₆ to polyaromatic hydrocarbons, are listed in Figure 4-5 at the optimal experimental conditions (650°C, 1.72 MPa, and 20:1 catalyst-to-lignin ratio) with their respective yields from HZSM-5 and Pd/HZSM-5 catalysts.

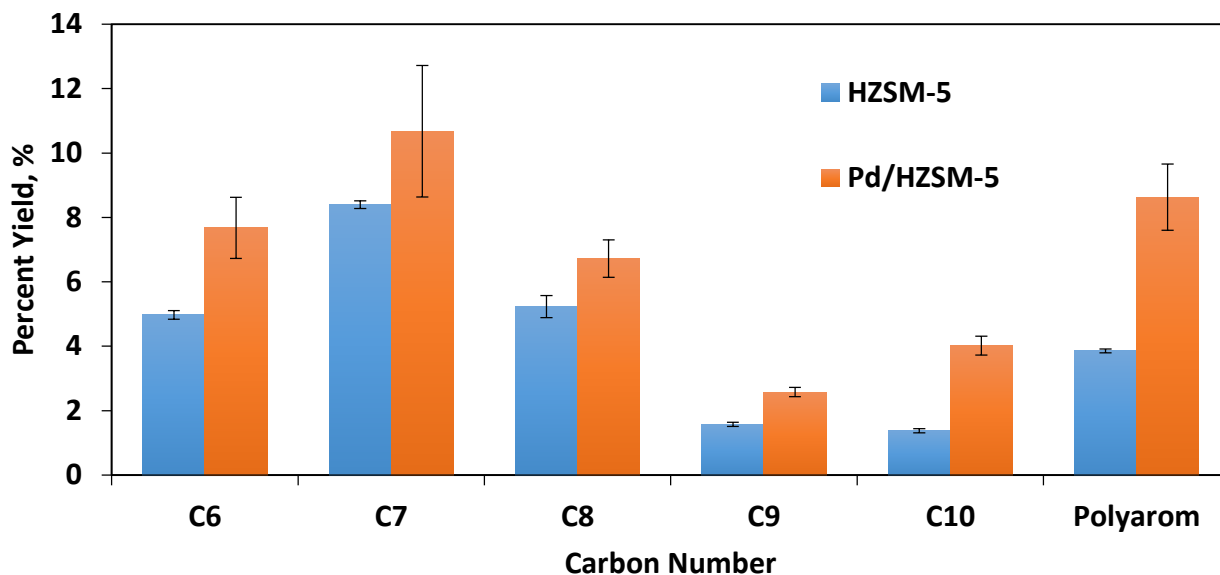


Figure 4-5. Aromatic hydrocarbon distribution over HZSM-5 and Pd/HZSM-5 at 650°C, $P_H=1.72$ MPa, and 20:1 catalyst-to-lignin ratio

Both catalysts, at the specified conditions, exhibited enhanced reactivity at 1.72 MPa. Pd/HZSM-5, however, produced more C6, C7, C8, C9, C10, and polyaromatic hydrocarbons than HZSM-5. This result is consistent with Figure 4-2 as Pd/HZSM-5 produced 44% more aromatic hydrocarbons than that of HZSM-5, with overall yields of approximately 40 wt.% and 26 wt.%, respectively. In particular, the toluene yield with Pd/HZSM-5 was 10.7 wt.%, a 27% increase compared to HZSM-5, which produced 8.4 wt.%. Xylene demonstrated a similar 28% increase with Pd/HZSM-5, with yields increasing from 5 wt.% to 7 wt.%. This result is critical as both toluene and xylene are commercially valuable products in both the fuel and chemical industries.

Naphthalenes and methylnaphthalenes, grouped in “Polyarom”, were major products formed from lignin over Pd/HZSM-5. In fact, the addition of Pd resulted in an astounding 123% increase in polyaromatic hydrocarbons compared to HZSM-5 itself. As polyaromatic hydrocarbons are generally known as precursors to char formation, this result may suggest that

the addition of Pd metal impedes char formation as these smaller ordered polyaromatic compounds were analyzed by a downstream GC/MS. For HZSM-5, it is possible that the polyaromatic compounds that were produced further reacted to form highly condensed species, otherwise known as char.

Our results suggest that Pd/HZSM-5 in H₂ conditions minimizes char agglomeration through in-situ interactions of aryl radicals with the Pd metal and H₂ atmosphere. Rapid polymerization of aryl radicals amongst neighboring aryl radicals may be inhibited by hydrogen atoms that are facilitated by the surface chemistry of the Pd metal, nullifying the formation of higher ordered polyaromatic rings, and increasing the yield of smaller polyaromatics.

4.3.4. Effect of Temperature

Typical hydrolysis processes occur from a range of 400°C to 600°C. This study focused on the effect of temperature (400°C, 550°C, and 650°C) and the product distribution from lignin hydrolysis over Pd/HZSM-5. Primarily, this study was performed to investigate the role of temperature on the formation of cycloalkane compounds. Catalyst ratio and pressure were held constant for all experiments at 20:1 and 1.72 MPa, respectively, as these conditions displayed improved aromatization from the previous results.

Figure 4-6 represents the product distribution resulting from the hydrolysis of poplar lignin at 400°C. The peaks were identified as cycloalkane compounds.

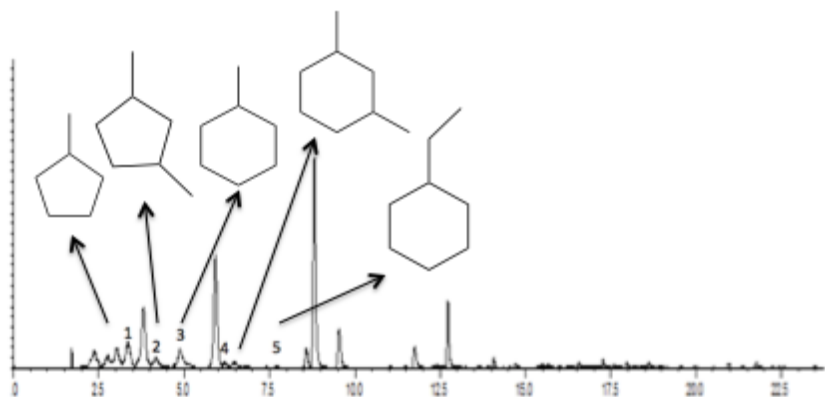


Figure 4-6. Chromatogram of catalytic hydropyrolysis of lignin at 400°C using Pd/HZSM-5

Figure 4-7 depicts the percent yield of aromatic and cycloalkane compounds at 400°C, 550°C, and 650°C. Five distinct cycloalkane species (methylcyclopentane, dimethylcyclopentane, methylcyclohexane, dimethylcyclohexane, ethylcyclohexane) appeared at 400°C. Although the total cycloalkane yield is 3 wt.%, this result indicates that Pd/HZSM-5 successfully facilitated HDO reactions of phenolic compounds or aromatics into cycloalkanes. In addition, no phenolic compounds were detected in the product distribution. As far as we know, this is the first time that cycloalkanes have been produced from natural lignin. The presence of cycloalkanes also demonstrates the bifunctionality of the Pd/HZSM-5 in hydropyrolysis conditions, since both the deoxygenation and hydrogenation reactions are needed to produce these molecules.

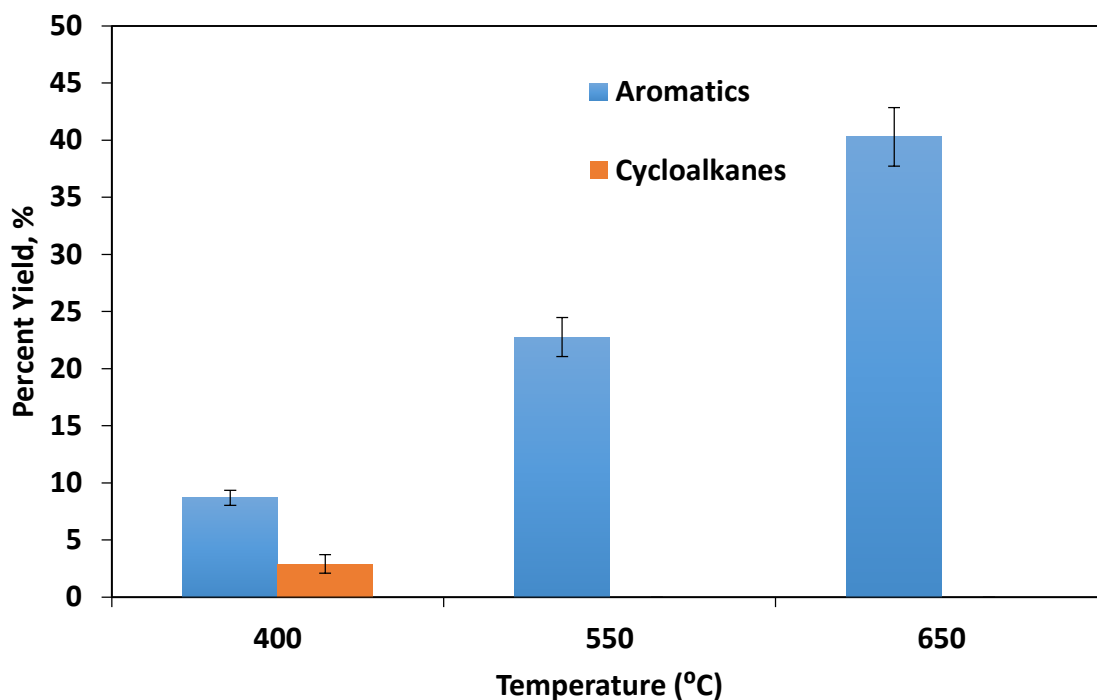


Figure 4-7. Aromatic and cycloalkane yields with Pd/HZSM-5 at 400°C, 550°C, and 650°C at $P_H=1.72$ MPa

Several studies on lignin model compounds have indicated that noble metals supported with an acidic support proceed via an initial hydrogenation (HYD) stage to remove the aromatization of the ring structure. A subsequent deoxygenation (DDO) step of the remaining C-O bond yields the resulting cycloalkane [13]. Hong et. al. analyzed the HDO of phenol using a Pt/HY bifunctionalized catalyst in a fixed bed reactor under elevated H_2 pressure (4MPa) with moderate reaction temperatures. The authors proposed that the successful HDO of phenol to cyclohexane occurred through a series of competing HYD/DDO reactions to yield cyclohexanol, followed with dehydration to eventually form cyclohexane [14]. The two competing mechanisms are represented in Figure 4-8, as adapted from Wang et. al [13].

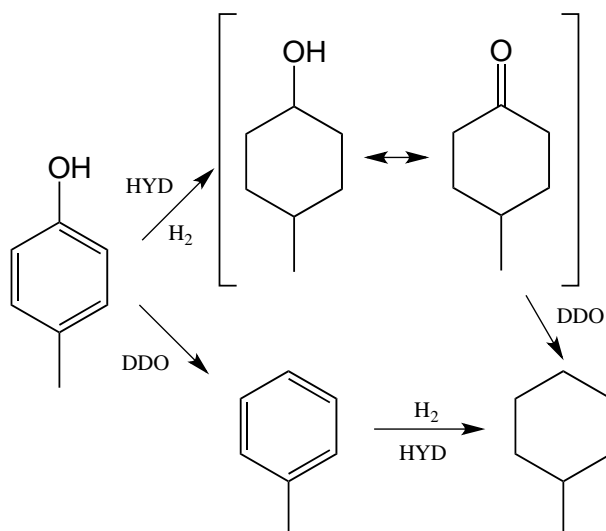


Figure 4-8. Hydrodeoxygenation reaction network of p-cresol to methylcyclohexane, adapted from Wang et. al.

Zhao and Lercher experimented with Ni/HZSM-5 catalysts to upgrade phenolic-rich bio-oil in a semi-batch reactor at 250°C. They observed that, with the addition of H₂ (5 MPa), Ni/HZSM-5 facilitated complete hydrodeoxygenation of phenolic monomers and dimers into cycloalkane molecules [15]. Wan et. al. observed that the orientation of the adsorbed molecule on the active site determined whether or not the reaction proceeded first via HYD or DDO. Cresol that was vertically adsorbed to the metal surface was more susceptible to DDO, resulting in toluene. HYD was proposed to be the major reaction pathway when cresol is adsorbed coplanar to the metal surface, resulting in methylcyclohexanol and subsequently methylcyclohexane [16]. Although the analysis of specific reaction mechanisms inherent with raw lignin hydrolysis is complex, it is suggested that Pd/HZSM-5 behaves in a similar catalytic fashion as observed from the model compound analyses.

As the hydrolysis temperature increased from 400°C to 650°C, cycloalkanes were no longer observed. The complimentary hydrogenation reactions appeared to be severely affected by the increase in temperature. This may be due to thermodynamic limitations, as hydrogenation

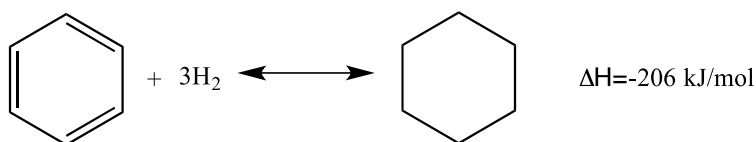
reactions are exothermic. As a result, the aromatic yield increases dramatically from 8.7 wt.% at 400°C to 40.3 wt.% at 650°C. Higher temperatures have been observed to improve the overall yields in the hydropyrolysis of the lignin, allowing for an increase in the amount of volatile vapor produced, which lead to increased overall yields.

Thangalazhy-Gopakumar et. al. performed similar studies but with an experimental design that kept the hydropyrolysis temperature constant at 650°C. Their results showed no formation of cycloalkane compounds at any H₂ partial pressure (0-400 psig) for any of the four supported catalysts that they used [4]. This is consistent with the result that we observed. This phenomenon is likely due to the low equilibrium constants of hydrogenation reactions at increasing temperatures, as summarized in Table 4-2. All equilibrium constants except those at 550°C and 650°C were reported literature values, with corresponding reaction enthalpy values for benzene, toluene, and p-xylene hydrogenation [17]. Equilibrium constants at 550°C and 650°C were calculated using the following equation, with 200°C as the reference temperature [18].

$$K_c(T) = K_c(T_1) \exp \left[\frac{\Delta H_{Rx}^o}{R} \left(\frac{1}{T_1} - \frac{1}{T} \right) \right] \quad (1)$$

The exothermicity of the hydrogenation reaction is accompanied by a decrease in product moles; high H₂ partial pressures and low temperatures would therefore favor optimal equilibrium conversion [19]. This trend is apparent in Figure 4-9, with the equilibrium constants for the hydrogenation of benzene, toluene, p-xylene, plotted with respect to temperature. Straight lines between points were included for better visualization. The decreasing equilibrium constant indicates that very few cycloalkane molecules will be produced at higher reaction temperatures [17]. The equilibrium constant for benzene hydrogenation to cyclohexane at 300°C is more than

21,000 times that of the constant at 650°C, meaning infinitesimal amounts of cyclohexane will be present, if any at all, at this higher temperature.



$\log_{10}K_{eq}$

Compound	200°C	300°C	400°C	550°C*	650°C*	ΔH°_{rxn}
Benzene	3.94	-0.13	-2.69	-5.73	-7.15	-206
Toluene	3.54	-0.19	-2.71	-6.08	-7.49	-205
p-xylene	2.16	-1.37	-3.75	-6.99	-8.33	-195

Table 4-2. Equilibrium constants for aromatics hydrogenation to cyclohexane. Enthalpy of reaction measured in kJ/mol. *calculated using equation 1.

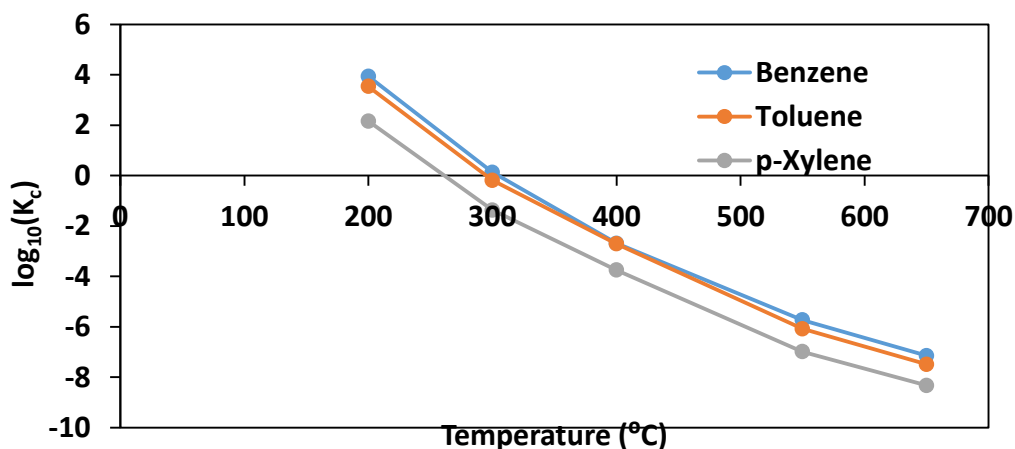


Figure 4-9. Equilibrium constants for hydrogenation of various aromatic hydrocarbons [17]

We observed no formation of cycloalkanes at 650°C, which is consistent to the findings of Thangalazhy-Gopakumar et. al. However, by decreasing the temperature to 400°C and maintaining a moderate H_2 partial pressure, the hydrogenation reactions favor cycloalkanes.

4.4 Ex-situ hydrolysis of lignin

Ex-situ hydrolysis of lignin was performed using the pyroprobe and packed bed reactor to determine any differences between in-situ and ex-situ upgrading. Approximately 0.5 mg of lignin was loaded in a quartz tube in the pyroprobe. A packed bed reactor downstream from the pyroprobe was packed with quartz wool and loaded with approximately 10 mg of catalyst. Fresh catalyst was used for each run. The hydrogen partial pressure and hydrolysis temperature were held constant at 1.72 MPa and 650°C respectively. The temperature of the packed bed reactor was tested at 300°C, 400°C, 500°C, 600°C, and 700°C; these temperatures represent the temperature on the outside of the reactor. The actual internal reactor temperature was not measured directly, as the heater and corresponding thermocouple were located on the exterior of the reactor.

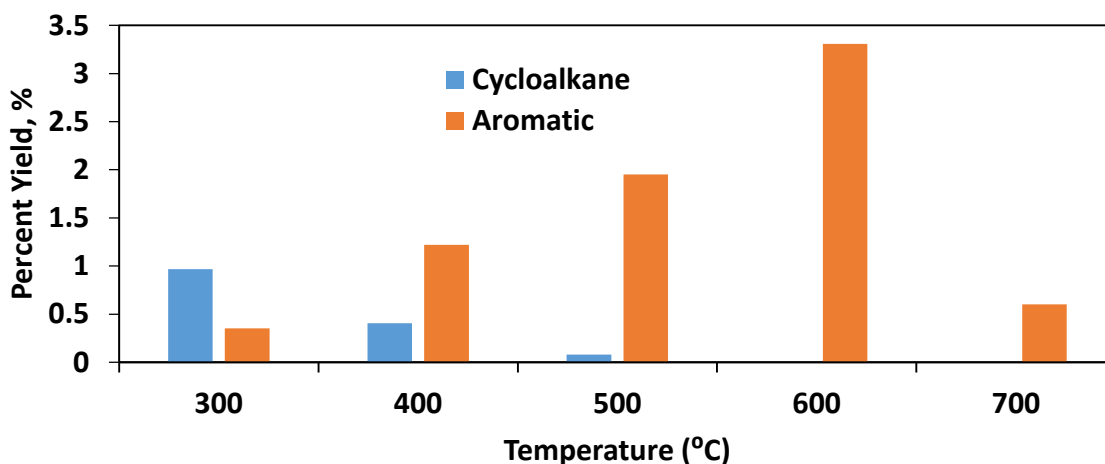


Figure 4-10. Ex-situ upgrading of lignin into cycloalkane and aromatic compounds with Pd/HZSM-5 at varying packed bed reactor temperatures. Hydrogen partial pressure = 1.72 MPa, approximately 20:1 catalyst to lignin ratio held constant

58% decrease in cycloalkane yield to 0.40 wt.% with a nearly 249% increase in aromatic yield, which is consistent with the exothermicity of the hydrogenation reaction discussed previously.

4.5 References

- [1] M. Zhang, F. L. P. Resende, and A. Moutsoglou, "Catalytic fast pyrolysis of aspen lignin via Py-GC/MS," *Fuel*, vol. 116, pp. 358–369, Jan. 2014.
- [2] C. A. Mullen and A. A. Boateng, "Catalytic pyrolysis-GC/MS of lignin from several sources," *Fuel Process. Technol.*, vol. 91, no. 11, pp. 1446–1458, Nov. 2010.
- [3] T. Carlson, G. Tompsett, W. Conner, and G. Huber, "Aromatic Production from Catalytic Fast Pyrolysis of Biomass-Derived Feedstocks," *Top. Catal.*, vol. 52, no. 3, pp. 241–252, 2009.
- [4] S. Thangalazhy-Gopakumar, S. Adhikari, and R. B. Gupta, "Catalytic Pyrolysis of Biomass over H + ZSM-5 under Hydrogen Pressure," *Energy & Fuels*, vol. 26, no. 8, pp. 5300–5306, Aug. 2012.
- [5] W. Yu, Y. Tang, L. Mo, P. Chen, H. Lou, and X. Zheng, "One-step hydrogenation-esterification of furfural and acetic acid over bifunctional Pd catalysts for bio-oil upgrading," *Bioresour. Technol.*, vol. 102, no. 17, pp. 8241–6, Sep. 2011.
- [6] M. Zahmakiran and S. Ozkar, "Metal nanoparticles in liquid phase catalysis; from recent advances to future goals," *Nanoscale*, vol. 3, no. 9, pp. 3462–81, Sep. 2011.
- [7] M. Zahmakiran, Y. Román-Leshkov, and Y. Zhang, "Rhodium(0) nanoparticles supported on nanocrystalline hydroxyapatite: highly effective catalytic system for the solvent-free hydrogenation of aromatics at room temperature," *Langmuir*, vol. 28, no. 1, pp. 60–64, Jan. 2012.
- [8] X. Zhu, L. L. Lobban, R. G. Mallinson, and D. E. Resasco, "Bifunctional transalkylation and hydrodeoxygenation of anisole over a Pt/HBeta catalyst," *J. Catal.*, vol. 281, no. 1, pp. 21–29, Jul. 2011.
- [9] S. a. Nikolaev, a. V. Chistyakov, M. V. Chudakova, E. P. Yakimchuk, V. V. Kriventsov, and M. V. Tsodikov, "Novel gold catalysts for the direct conversion of ethanol into C3+ hydrocarbons," *J. Catal.*, vol. 297, pp. 296–305, Jan. 2013.
- [10] P. Treesukol, K. Srisuk, J. Limtrakul, and T. N. Truong, "Nature of the metal-support interaction in bifunctional catalytic Pt/H-ZSM-5 zeolite," *J. Phys. Chem. B.*, vol. 109, no. 24, pp. 11940–5, Jun. 2005.
- [11] Y.-T. Cheng, J. Jae, J. Shi, W. Fan, and G. W. Huber, "Production of renewable aromatic compounds by catalytic fast pyrolysis of lignocellulosic biomass with bifunctional Ga/ZSM-5 catalysts," *Angew. Chem. Int. Ed. Engl.*, vol. 51, no. 6, pp. 1387–90, Feb. 2012.

- [12] C. Zhao and J. a Lercher, "Upgrading pyrolysis oil over Ni/HZSM-5 by cascade reactions.," *Angew. Chem. Int. Ed. Engl.*, vol. 51, no. 24, pp. 5935–40, Jun. 2012.
- [13] H. Wang, J. Male, and Y. Wang, "Recent Advances in Hydrotreating of Pyrolysis Bio-Oil and Its Oxygen-Containing Model Compounds," *ACS Catal.*, vol. 3, no. 5, pp. 1047–1070, May 2013.
- [14] D.-Y. Hong, S. J. Miller, P. K. Agrawal, and C. W. Jones, "Hydrodeoxygenation and coupling of aqueous phenolics over bifunctional zeolite-supported metal catalysts.," *Chem. Commun. (Camb)*, vol. 46, no. 7, pp. 1038–40, Feb. 2010.
- [15] C. Zhao and J. a. Lercher, "Selective Hydrodeoxygenation of Lignin-Derived Phenolic Monomers and Dimers to Cycloalkanes on Pd/C and HZSM-5 Catalysts," *ChemCatChem*, vol. 4, no. 1, pp. 64–68, Jan. 2012.
- [16] H. Wan, R. V. Chaudhari, and B. Subramaniam, "Catalytic Hydroprocessing of p-Cresol: Metal, Solvent and Mass-Transfer Effects," *Topics in Catalysis*, vol. 55, pp. 129–139, 2012.
- [17] J. Ancheyta and J. G. Speight, *Hydroprocessing of Heavy Oils and Residua*. 2007.
- [18] H. S. Fogler, *Elements of Chemical Reaction Engineering*. 2006.
- [19] B. C. Gates, *Catalytic Chemistry*. Wiley Series in Chemical Engineering, 1992.

CHAPTER 5 THESIS SUMMARY AND FUTURE WORK

5.1 *Thesis Summary*

The hydropyrolysis of lignin was performed with HZSM-5 and Pd/HZSM-5 to assess the hydrodeoxygenation of lignin-derived phenolics to aromatic hydrocarbons and cycloalkanes. One of the key findings was that Pd/HZSM-5 produced 44% more aromatic hydrocarbons than HZSM-5 at a catalyst-to-lignin ratio of 20:1, H₂ partial pressure of 1.72 MPa, and hydropyrolysis temperature set to 650°C. The most abundant aromatic hydrocarbons were toluene, xylene, and polyaromatic compounds such as naphthalene and methylnaphthalene. These results appear to indicate that Pd/HZSM-5 may be a more active catalyst for aromatization and cyclization reactions in contrast to other previous iterations of supported Co, Ni, Mo, and Pt catalysts. The hydropyrolysis temperature was shown to affect the yields of cycloalkanes over Pd/HZSM-5 in H₂ through thermodynamic limitations. The yield of cycloalkanes from ex-situ catalytic upgrading appeared to be affected by thermodynamic limitations as well, with similar trends to in-situ upgrading. Although the yield of cycloalkanes is low, this result provides evidence that the bifunctional catalyst was successful in facilitating hydrodeoxygenation reactions of phenolic compounds into cycloalkanes. Further experimentation with inexpensive catalysts and HZSM-5 support may elucidate other effective bifunctional catalysts for HDO of natural lignin.

5.2 *Future work*

Along with the pyroprobe experiments presented in the previous chapters, I constructed and assembled two laboratory-scale reactors in Bloedel 108. These two reactors will be used to gather experimental data on biomass hydrolysis and ethylene to jet fuel processes respectively. Each system is described in the following sections.

5.2.1 Hydrolysis system

The work in this thesis was performed to test the viability of forming cycloalkanes through hydrolysis of lignin by using a zeolite support in conjunction with a hydrogenation metal catalyst. This work was conducted on a microscale pyroprobe system where only minute amounts (~0.5 mg) of biomass could be introduced into the system. A larger system is currently being assembled, and it will feature a screw auger feeder for biomass delivery, a hydrogen manifold with both low and high pressure options, a fluidized bed reactor, a cyclone for vapor-solid separation, and condensers for liquid bio-oil collection.

The proposed hydrolysis system will extend the results of this thesis work to the laboratory-scale, with a biomass throughput of 2 kg/hour. A simplified process flow diagram is shown below in Figure 5-1. The system is designed to handle a wide range of pressure from atmospheric to as high as 1000 psig of hydrogen. The fluidized bed reactor will be operated from 400°C to 600°C, with four thermocouple ports to measure the temperature throughout the fluidized bed. A gas booster is included in the design to recirculate the excess hydrogen gas back into the system as a recycle loop. This gas booster will help reduce hydrogen consumption.

The catalysts make up the bed of particles in the reactor. Future work with this system will look into several types of bifunctional catalysts with several hydrogenation metals. More affordable metals, such as Ni, Co, and Fe, with HZSM-5 and other supports will be tested to attempt to improve the quality of the bio-oil, examine improvements in turnover frequency, and determine which catalysts may be viable candidates for industrial scale-up.

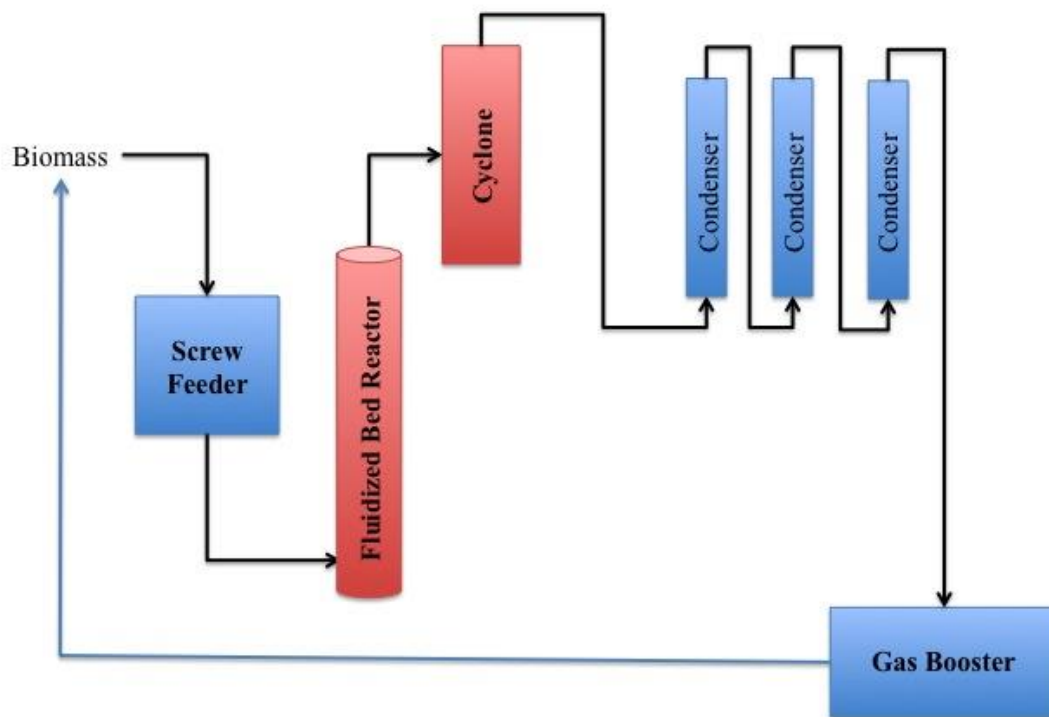


Figure 5-1. Hydrolysis system PFD

Figures 5-2 through 5-5 are pictures of the physical components of the hydrolysis system in Bloedel 108. The frame is constructed of 80/20 aluminum bars. All components are composed of stainless steel 316 and are precision-machined and high-pressure welded by Wheeler Tank Manufacturing in Sioux Falls, SD.



Figure 5-2. Overall hydrolysis system complete with screw feeder, hydrogen manifold, gas booster

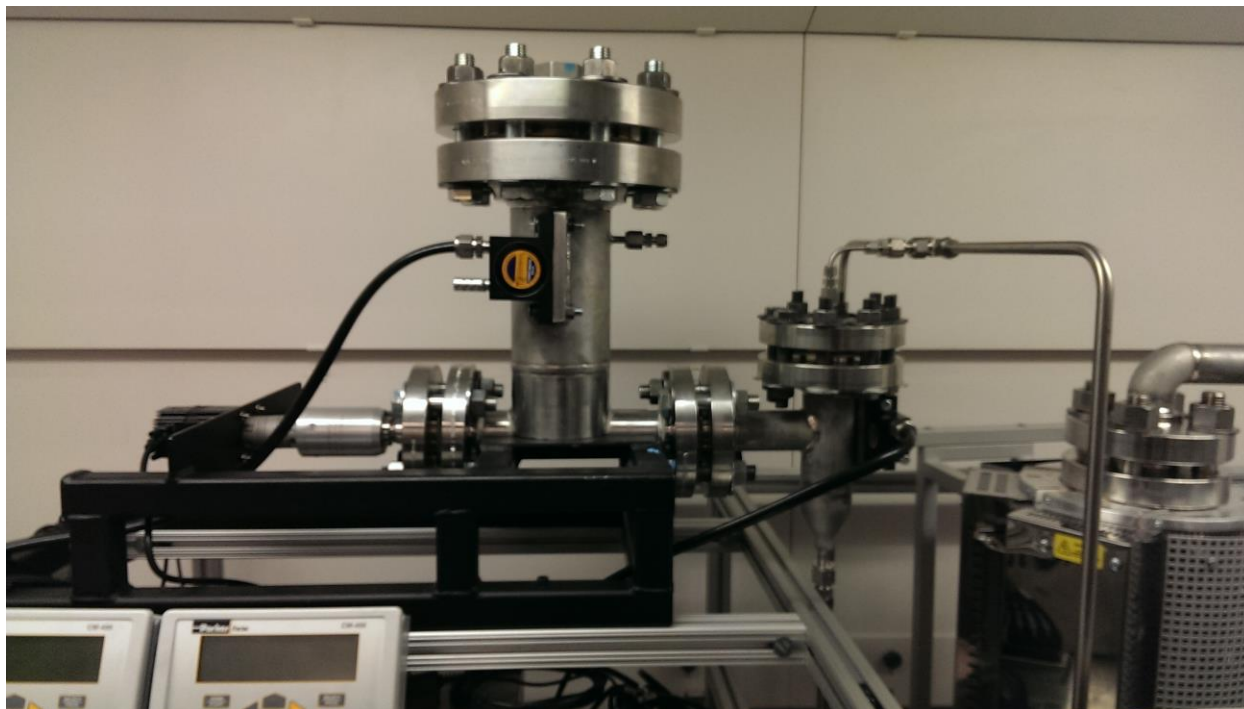


Figure 5-3. Biomass screw feeder and rotating auger with funnel and vibrating tabs

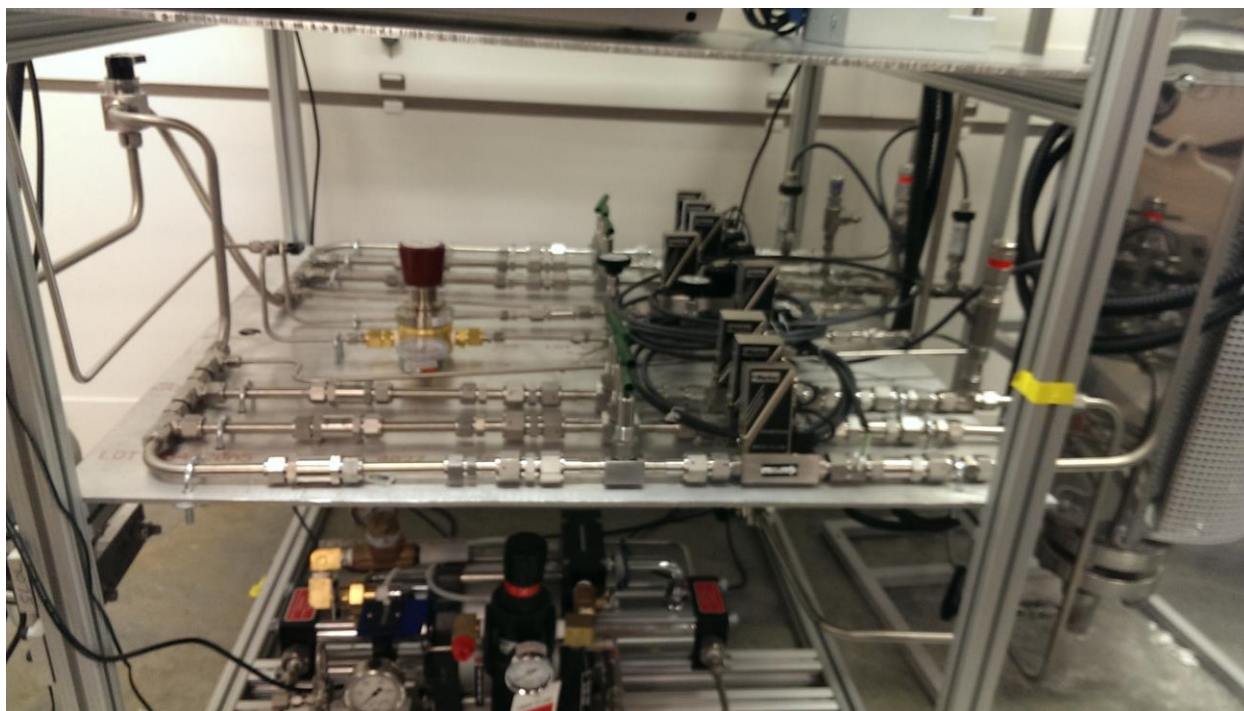


Figure 5-4. Hydrogen gas manifold with both low and high-pressure options



Figure 5-5. Fluidized bed reactor with vertical tube furnace connected to cyclone.

5.2.2 Ethylene-to-jet fuel system

Along with the hydrolysis system, I was also responsible with setting up another catalytic reactor for the conversion of ethylene to jet fuel. This reactor will be used to study the oligomerization of gaseous ethylene into hydrocarbons suitable for use in jet fuels. The system consists of a packed bed reactor along with a condenser for liquid hydrocarbon collection. The PFD is shown in Figure 5-2.

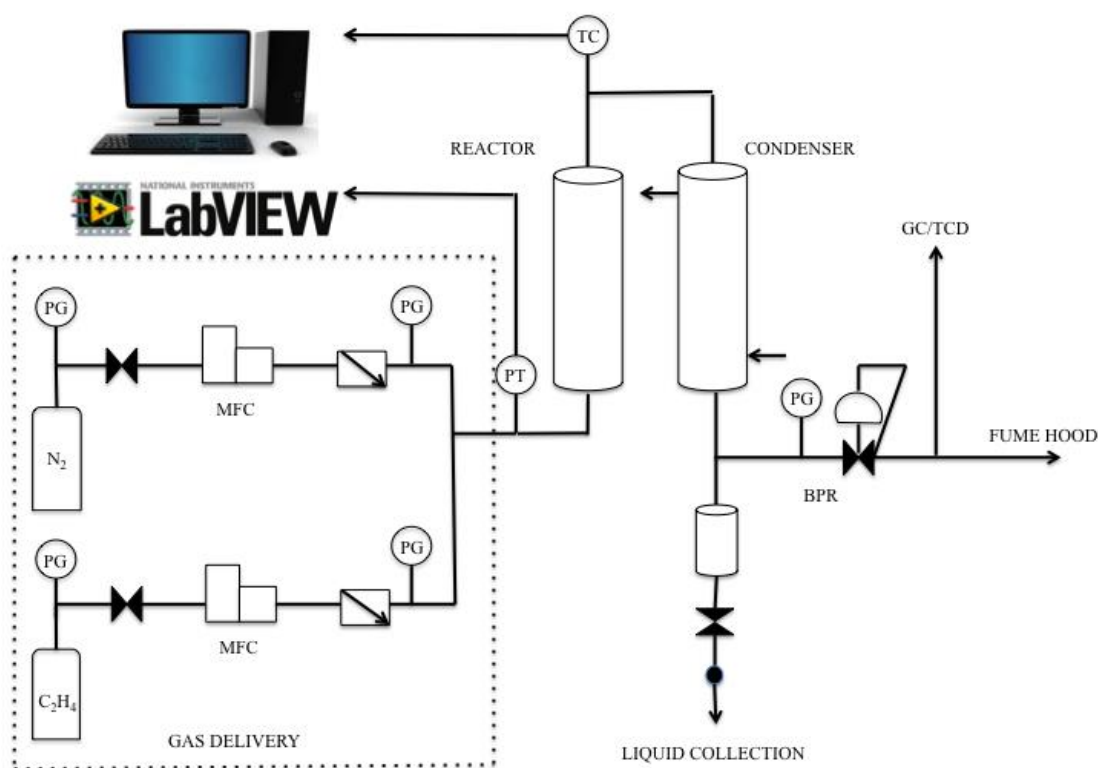


Figure 5-6. Ethylene to jet fuel PFD

Nitrogen will be used as a carrier gas throughout the process, whereas ethylene will be the sole reactant. The gas delivery system consists of an ethylene and a nitrogen gas line, both equipped with mass flow controllers and pressure gauges. Pressure in the system will be limited to 1000 psig and will be controlled using a backpressure regulator. Heating tape will be used to

heat the reactor walls, with a top-mounted thermocouple inserted into the packed bed for online temperature readings on the internal reactor temperature. The catalyst will be supported by a layer of quartz wool on both sides of the packed bed. A pressure transducer right before the packed bed reactor and a downstream pressure gauge will be used to measure pressure drop across the reactor. The vapors from the reactor will be swept into a condenser operating in counterflow at 5°C to condense the vapors into a liquid that will be analyzed by GC-MS/FID. Permanent gases will be swept either into a gas-sampling bag or measured online periodically using GC-TCD.

This project will focus on catalyzing oligomerization reactions of ethylene into higher-ordered alkanes that are suitable for jet fuels. We will look at utilizing interesting polymerization catalysts (i.e. Ziegler-Natta and Philips catalysts) along with acidic supports to achieve this goal. These catalysts typically consist of alkylated titanium and/or chromium nanoparticles dispersed on an inert support for industrial polyethylene production [1]. The idea is to use an acidic support (i.e. zeolites) in conjunction with these productive catalysts that can catalytically crack oligomeric ethylene into suitable paraffins and olefins while also restricting polymerization reactions from occurring. In addition, using zeolites may also accelerate transalkylation reactions that can form important branched paraffins/olefins [2].

In addition to the catalyst studies, supercritical conditions ($T_r > 1$, $P_r > 1$) will be tested to see if coke formation on catalytic sites can be reduced. By reducing coke formation, catalyst lifetime can be extended with the added benefit of requiring fewer regeneration cycles and improved turnover frequency.

The physical reactor system is shown in Figure 5-7, with the packed bed reactor on the left connected to an adjacent condenser.

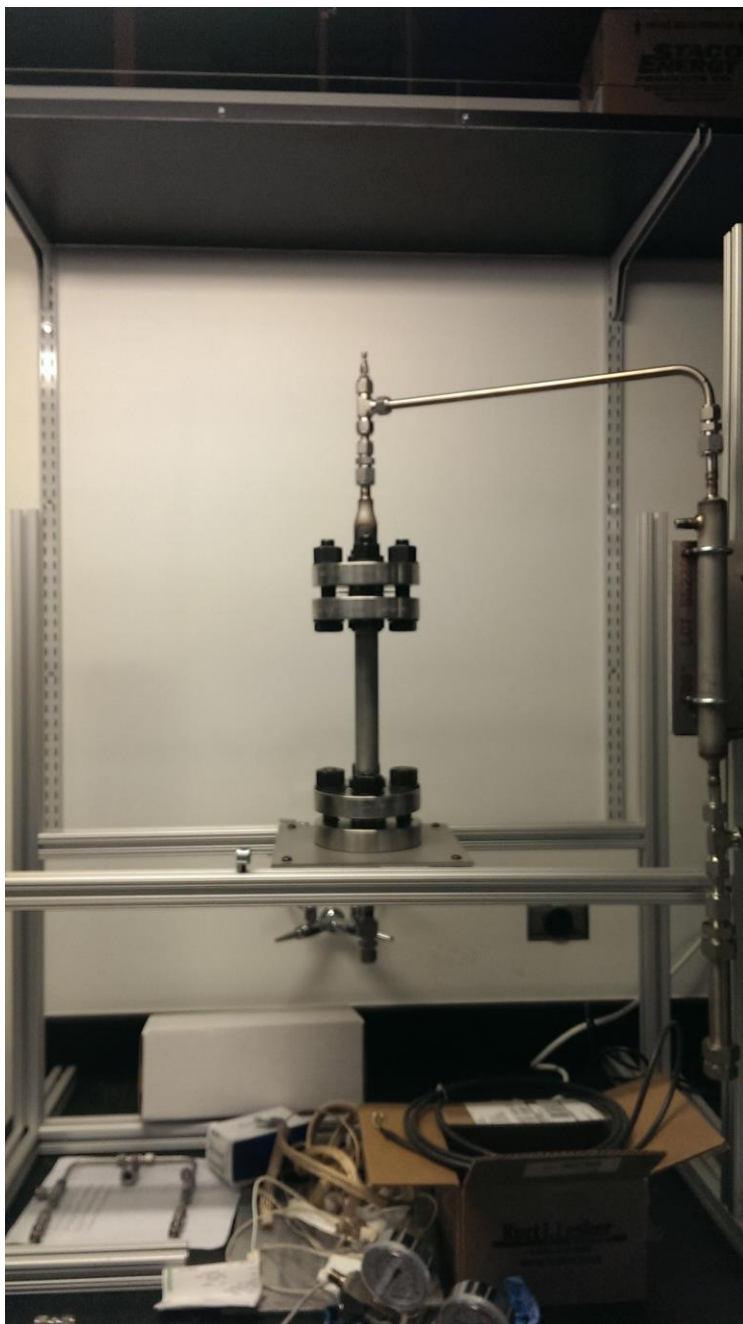


Figure 5-7. ETG reactor system

5.3 References

- [1] G. P. Chiusoli and P. M. Maitlis, *Metal-catalysis in Industrial Organic Processes*. RSC Publishing, 2006.
- [2] X. Zhu, R. G. Mallinson, and D. E. Resasco, “Role of transalkylation reactions in the conversion of anisole over HZSM-5,” *Appl. Catal. A Gen.*, vol. 379, no. 1–2, pp. 172–181, May 2010.